Pseudorotaxanes Formed between Secondary Dialkylammonium Salts and Crown Ethers**

Peter R. Ashton, Ewan J. T. Chrystal, Peter T. Glink, Stephan Menzer, Cesare Schiavo, Neil Spencer, J. Fraser Stoddart,* Peter A. Tasker, Andrew J. P. White, and David J. Williams

Abstract: A very simple self-assembling system, which produces inclusion complexes with pseudorotaxane geometries, is described. The self-assembly of eight pseudorotaxanes with a range of stoichiometries—1:1, 1:2, 2:1, and 2:2 (host:guest)—has been achieved. These pseudorotaxanes self-assemble from readily available components—well-known crown ethers, such as dibenzo[24]crown-8 and bis-*p*-phenylene[34]crown-10, and secondary dialkylammonium hexafluorophosphate salts, such as $(PhCH_2)_2NH_2^+PF_6^-$ and $(n\text{Bu})_2NH_2^+PF_6^-$—and have been characterized not only in the solid state, but also in solution and in the "gas phase". The pseudorotaxanes are stabilized largely by hydrogen-bonding interactions and, in some instances, by aryl–aryl interactions.

Keywords
crown ethers · dialkylammonium salts · hydrogen bonding · molecular recognition · pseudorotaxanes · self-assembly

Introduction

In his seminal paper published in 1967 on the complexing ability of some crown ethers with a variety of cations,[1] Pedersen noted that, although primary alkylammonium ions (RNH_3^+) form 1:1 complexes with dibenzo[18]crown-6 (**DB18C6**), secondary dialkyl- ($R_2NH_2^+$) and tertiary trialkyl- (R_3NH^+) ammonium ions do not bind to this macrocyclic polyether. He concluded that "apparently, $[RNH_3^+]$ can intrude sufficiently into the polyether ring of **[DB18C6]** to affect its spectrum but, due to steric hindrance, $[R_2NH_2^+]$ and $[R_3NH^+]$ cannot do so" (Fig. 1). In the intervening decades since this observation was made, the complexation[2] of primary alkylammonium salts with crown ethers has become one of the major areas of development in supramolecular chemistry[3] with applications ranging from ion transport through membranes[4] to the resolution of racemic mixtures of chiral primary alkylammonium salts.[2e, 2m, 5]

The conformations of [18]crown-6 (**18C6**) derivatives are close to ideal for binding ammonium[6] and primary alkylammonium[7] ions. For example, the simplest system, **18C6** itself,

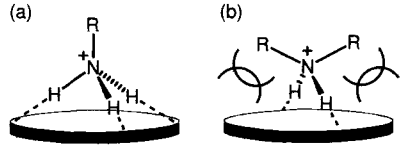

Fig. 1. Diagrammatic representations of a) the three-point binding of a primary alkylammonium ion (RNH_3^+) with **18C6** and b) the two-point binding of a secondary dialkylammonium ion ($R_2NH_2^+$) with **18C6.**

usually adopts a preferred complexing conformation in the solid[2] and solution[8] states with local D_{3d} symmetry in which the six oxygen atoms are arranged alternately above and below the mean plane of the macrocycle. The binding of ammonium and primary alkylammonium ions by **18C6** almost always occurs in a face-to-face manner, with $[N-H\cdots O]$ hydrogen bonding in an alternating mode with respect to the six oxygen atoms.[2] The most common complexes have a *perched*[9] geometry—that is, the oxygen atoms involved in hydrogen bonding are those positioned on the side of the macrocycle facing the RNH_3^+ ion (Fig. 2). In a few exceptional cases, such as in the 1:1 complex formed with hydrazinium perchlorate,[7c] the hydrogen bonding occurs, in the solid state at least, in a *nested*[9] arrangement, wherein the oxygen atoms positioned on the opposite face of the macrocycle with respect to the ion are the ones that become involved in the primary hydrogen-bonding interactions. Considerable contributions to the stability of these complexes are made

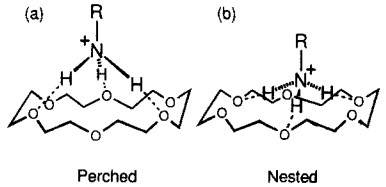

Fig. 2. Diagrammatic representations of a) the perched and b) the nested geometries found in the solid state for the binding of primary alkylammonium ions with **18C6** in its D_{3d} conformation.

[*] Prof. J. F. Stoddart, Dr. P. T. Glink, Dr. N. Spencer, C. Schiavo, P. R. Ashton
School of Chemistry, The University of Birmingham
Edgbaston, Birmingham B152TT (UK)
Fax: Int. code +121-414-3531
Dr. E. J. T Chrystal
ZENECA Agrochemicals, Jealott's Hill Research Station
Bracknell, Berkshire RG1 6EY (UK)
Dr. P. A. Tasker
ZENECA Specialties, P.O.Box 42, Hexagon House
Blackley, Manchester M9 3DA (UK)
Dr. D. J. Williams, Dr. S. Menzer, Dr. A. J. P. White
Chemical Crystallography Laboratory, Department of Chemistry
Imperial College, South Kensington, London SW72AY (UK)

[**] "Molecular Meccano", Part 6: for Part 5, see ref. [45e].

by the non-hydrogen-bonding oxygen atoms which are involved in other ion–dipole interactions with the ammonium center. As Pedersen deduced right back at the infancy of crown ether chemistry, it is the deep "intrusion" of the ammonium ion into the cavity of the crown that results in the most stable complexes being formed.[1] Trueblood extended this concept in the early 1980s[7c] by suggesting that "the primary factor governing the geometry of the interaction at the ether oxygen atoms is the depth of penetration of the -NH_3^+ group, irrespective of whether hydrogen bonding is involved." That is, it is the total positive charge associated with the ammonium ion, and not just that associated with the hydrogen atoms of the -NH_3^+ group, which the crown ether wishes to stabilize by accommodating as much of the ion as deeply as possible within its cavity. For **18C6**-sized macrocycles, however, total insertion of the ion generally is not possible for steric reasons—the cavity is simply too small for an ammonium center to penetrate. In addition, if total insertion did occur, disruption of the near-perfect hydrogen-bonding pattern (perched or nested face-to-face mode) could weaken the association. An optimal situation would allow for the total insertion of the ammonium center into the cavity of the crown with concomitant hydrogen bonding within that cavity. However, merely enlarging the size of the macroring often does not have the desired effect: lower association constants are often found for the complexation of RNH_3^+ ions by the larger-ring crown ethers.[10] Although considerable effort has been given over to the study of crown ethers larger than **18C6** with ammonium ions, most studies of primary alkylammonium ion binding have been concentrated on macrocycles that are derivatives of **18C6**.[10] It is generally accepted in the literature that an alkyl group requires a macrocycle consisting of at least 24 atoms before threading becomes possible.[11] Yet, studies of [24]crown-8, and larger, macrocyclic polyethers with primary alkylammonium ions is an area of investigation which has been largely neglected,[12] and crystal structures of such complexes[13] are rare. One noteworthy exception is the complex formed in the solid state between a furan-modified [24]crown-8 and benzylammonium perchlorate reported by Bradshaw and co-workers.[13c] Despite the fact that this complex exists (Fig. 3) in the crystal with the $CH_2NH_3^+$ group inserted deeply into the macrocycle, only two of its NH_3^+ hydrogen atoms are involved in hydrogen bonds with the crown ether oxygen atoms: the other hydrogen atom hydrogen bonds to the perchlorate counterion *through* the cavity of the macrocycle. In addition, the benzylic methylene hydrogen atoms are involved in [N^+–C–H···O] hydrogen bonds with the crown ether oxygen atoms. In this example, the ammonium center and the benzylic methylene group of the guest molecule have penetrated virtually into the center of the crown ether, consistent with Trueblood's statement.[7c] However, such a geometry cannot allow for three-point [N–H···O] hydrogen bonding by the ammonium group and so extra stability is gained by utilizing the slightly weaker [N^+–C–H···O] hydrogen bonds.

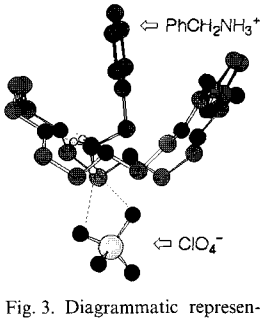

Fig. 3. Diagrammatic representation of the solid-state structure formed between a furano-modified **24C8** and benzylammonium perchlorate, described by Bradshaw and co-workers [13c]. Because of the size of the ring, hydrogen bonding can take place within the macrocycle's cavity, although only by two-point [N–H···O] hydrogen bonding. The third ammonium hydrogen atom interacts with the counterion through the ring, forming what may be likened to an "ion-pair pseudo[2]rotaxane".

In comparison with primary alkylammonium ion binding by crown ethers, there have been very few investigations carried out on the binding of secondary, or indeed tertiary, ammonium salts with macrocycles. Misumi and co-workers[14] have reported complexes formed between a phenol-[15] and a phenol/carboxylic acid-functionalized[16] dyed macrocycle (acerand) with a number of amines. The second of these macrocycles binds piperazine *within* the cavity of the macrocycle: the term "saltex" has been coined[16] to describe these salt complexes. Misumi's group has also shown that these dyed macrocycles exhibit amine-selective coloration upon "saltexation" such that the substitution pattern of the amine may be determined spectrophotometrically.[17] Additionally, Vögtle and Hoss have described a tetrahydroxycyclophane that binds selectively to a number of diamines[18]—possibly within the cavity, as suggested by marked ^{1}H NMR chemical shift changes upon "saltexation". More specifically, the binding of secondary dialkylammonium salts by simple crown ethers has been reported by a few research groups. We shall mention five examples:

1) Izatt et al. studied the binding of ammonium, primary alkylammonium, secondary dialkylammonium and tertiary trialkylammonium ions with **18C6** and determined that the association constants for these systems decrease in the order $RNH_3^+ > R_2NH_2^+ > R_3NH^+$, R_4N^+.[19]
2) In 1977 we reported that *N,N'*-dimethyl-1,7-diaza[12]crown-4 binds secondary dialkylammonium salts, such as dibenzylammonium thiocyanate, in solution with a face-to-face geometry by a two-point binding mechanism.[20]
3) Krane and Aune proposed a very similar geometry—although with a slightly different crown ether conformation—for the same systems.[21]
4) Tsukube has reported that diazacrown ethers derived from **15C5**, **18C6**, and **21C7** are effective as agents for the transport of the secondary amino acid derivative, proline methyl ester perchlorate, across a chloroform membrane.[22]
5) Brisdon and co-workers have prepared a polysiloxane, functionalized on its side chains with pendant [12]crown-4 groups, for the extraction of secondary dialkylammonium salts from a mixture of protonated secondary and tertiary amines.[23]

In all these cases, a two-point binding motif was suggested as the means of complexation using a face-to-face geometry (Fig. 4). Since the strongest complexes formed between primary alkylammonium ions and crown ethers have the alkylammonium ions penetrating deeply into the macrocycle's cavity, it seems logical to propose that secondary dialkylammonium ions would also prefer to complex with crown ethers in such a way as to place the NH_2^+ center within the plane of the macrocycle. This situation can only be achieved if the crown ether is of an appropriate size to allow the threading of an alkyl group through its cavity; that is, at least 24 atoms are required in the macrocyclic polyethers. Surprisingly, this simple proposition (Fig. 5) had, to our knowledge, never been tested experimentally—or, if it had, it had not been reported in the literature—at the time we launched our research program.

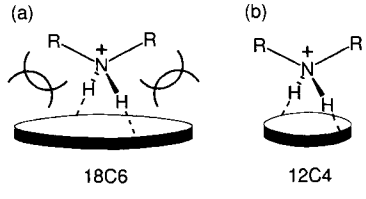

Fig. 4. Diagrammatic representations of the two-point binding of a secondary dialkylammonium ion ($R_2NH_2^+$) with a) **18C6** and b) **12C4**.

We have communicated recently that this proposition holds true to form:[24, 25] secondary dialkylammonium ions *do* complex with macrocyclic polyethers, such as **DB24C8** and

0947-6539/96/0206-0710 $ 15.00+.25/0 Chem. Eur. J. 1996, 2, No. 6

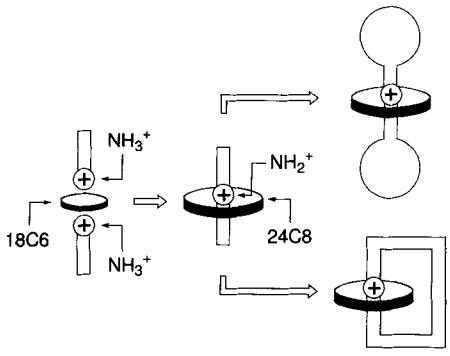

Fig. 5. A conceptual journey: If crown ethers could, electrostatic repulsion apart, accommodate two NH_3^+ centers perching on both faces of the macrocycle, would opening up the ring (i.e., increasing the size of the macrocycle) allow for the insertion of a secondary dialkylammonium ion? If so, could we utilize this interaction for the construction of mechanically interlocked molecules, such as rotaxanes and catenanes?

BPP34C10, to provide novel supramolecular entities and arrays stabilized predominantly by hydrogen bonding[26] within the crown ether cavity. The superstructures generated by the threading of secondary dialkylammonium salts through these macrocycles are those of the so-called pseudorotaxanes.[27] We,[28] and others,[29] have been interested in the pseudorotaxanes and their mechanically interlocked counterparts, the rotaxanes,[30] as supramolecular arrays and molecular assemblies, respectively, which have the potential in many fields of nanoscience, such as the nanoscale fabrication of devices,[31] like switches[32] and shuttles,[33] that are capable of being controlled by external physical or chemical stimuli. Also, during 1995, Busch and co-workers reported a [2]rotaxane formed between **DB24C8** and a dumbbell-shaped component incorporating a secondary dialkylammonium center.[34] An X-ray crystal structure determination performed on this compound reveals quite clearly the interaction of the dialkylammonium center with the crown ether, that is, hydrogen bonding occurs within the cavity of the macrocyclic polyether. We report in the paper following this one,[35] a number of rotaxanes incorporating secondary dialkylammonium ion centers as recognition sites for crown ether molecules.

In this paper, we wish to provide an overview of the extensive evidence we have accrued to date that pseudorotaxane geometries exist not only in the solid state, but also in solution and indeed in the "gas phase", for eight different complexes of varying stoichiometries involving four different dialkylammonium salts and three different crown ethers. In our coverage of these supramolecular systems, we compare and contrast the effects that changes made in the constitutions of these guest and host species have on the superstructures and dynamics of the complexes.

Results and Discussion

The dialkylammonium ions we have been studying in this program of research are simple in their constitutions, and the amines from which they are derived are either commercially available (**1**, **2**, **3**) or can be synthesized (**4**)[25] by using traditional chemistry. Similarly, the crown ethers we have investigated are either commercially available (**DB24C8**) or can be prepared (asym-**DB24C8**,[1] **BPP34C10**[12c, 36]) by standard literature procedures. The dialkylammonium ions have all been studied as their hexafluorophosphate salts: the PF_6^- counterions were chosen 1) so as to enhance the organic solubilities of the cations and 2) to weaken ion pairing, thus allowing strong binding by

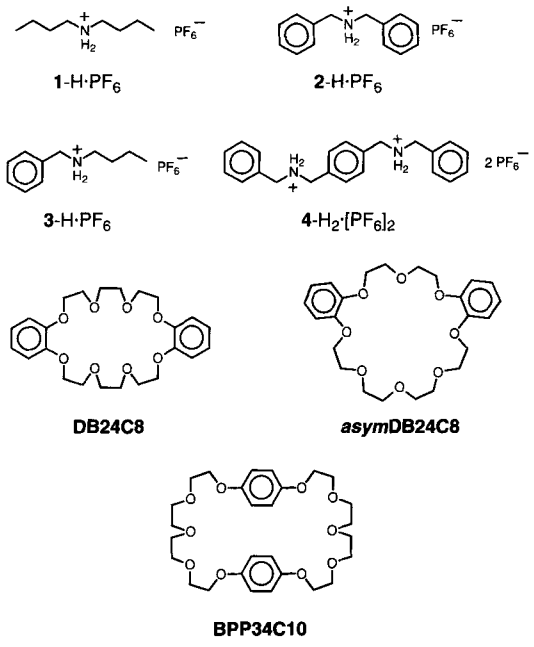

the macrocyclic crown ether ligands. The salts were all prepared readily from the corresponding hydrochloride salts by counterion exchange. We shall now discuss the nature of some eight complexes formed between these ions and macrocycles for which we have managed to obtain solid-state structures by X-ray crystallography.

1. Di-*n*-butylammonium Hexafluorophosphate (1-H·PF_6) and Dibenzo[24]crown-8 (DB24C8): Although **1**-H·PF_6 is soluble in solvents such as MeCN, Me_2CO, Me_2SO, and MeOH, it is virtually insoluble in $CHCl_3$ and CH_2Cl_2. However, solubility in these chlorinated solvents can be achieved in the presence of one or more molar equivalents of **DB24C8**. This observation was the first encouraging evidence we obtained that suggested that strong 1:1 complexation of some type could occur with these systems. Crystals of this complex were grown. The FAB mass spectrum revealed (Fig. 6) a peak at *m/z* 578 corresponding to a 1:1 complex having lost its PF_6^- counterion. This complex ion has an intensity of almost 20% of that observed for the base peak in the spectrum—that of the naked dialkylammonium ion **1**-H^+. In comparison, the peak (*m/z* 448) associated with the uncomplexed macrocycle has an intensity of less than 5% of the

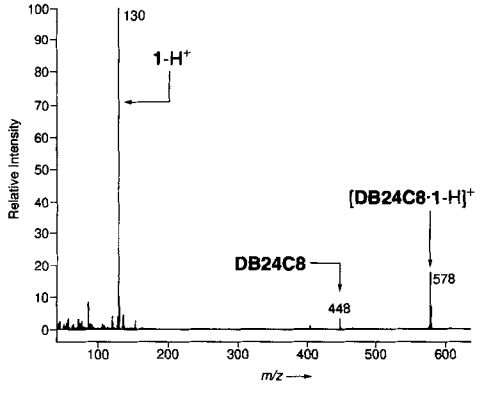

Fig. 6. The FAB mass spectrum of crystals grown of a 1:1 complex between **1**-H·PF_6 and **DB24C8**.

base peak's height.[37] This evidence suggests that the rate of decomplexation of this supramolecular system is far from being so fast as to occur totally during the time of flight of the complex through the spectrometer.

The solid-state structure of the complex was elucidated by X-ray crystallography on suitable single crystals. Gratifyingly, the complex exists (Fig. 7) with the geometry of a pseudorotaxane with 1:1 stoichiometry. The **DB24C8** component adopts an extended all-*gauche* conformation for the O-C-C-O units in its ethyleneglycol chains, and a substantial cavity is formed. The NH_2^+ center is positioned within this cavity and almost in the plane of the macrocycle. The ion and the crown ether are bound together by three major hydrogen bonds—two [N–H···O] contacts and one [N–C–H···O] contact. As is observed commonly[2, 7, 13] in the face-to-face complexation of primary alkylammonium ions with crown ethers, the oxygen atoms involved in the hydrogen bonding with NH_2^+ hydrogen atoms are nonadjacent ones; that is, they are separated by five atoms, including another oxygen atom. This 1,3-alternate arrangement of H-bond acceptors necessitates, for **DB24C8**, that the two [N^+–H···O] interactions occur with one aliphatic ether oxygen and one phenolic ether oxygen atom, respectively. In this complex, these two oxygen atoms are situated on different polyether chains, so the [O···H–N^+–H···O] network of bonds straddles a catechol subunit. This pattern is repeated in some of the other complexes we have observed with this crown ether (vide infra). The one [N–C–H···O] contact occurs with an aliphatic ether oxygen atom.[38] There are no dominant stabilizing interactions between these 1:1 complexes.

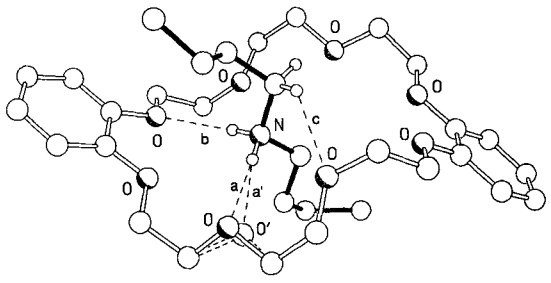

Fig. 7. The superstructure of the 1:1 complex [**DB24C8**·**1**-H]$^+$ in the solid state. The hydrogen bonds have the following distances and angles: a) [N···O] 3.09 Å, [H···O] 2.20 Å, [N–H···O] 175°; a') [N···O'] 2.90 Å, [H···O'] 2.04 Å, [N–H···O'] 161°; b) [N···O] 3.25 Å, [H···O] 2.35 Å, [N–H···O] 172°; c) [C···O] 3.23 Å, [H···O] 2.48 Å, [C–H···O] 134°.

The nature of the complexation was studied in solution by ^{1}H NMR spectroscopy. At room temperature in a number of solvents ($CDCl_3$, CD_3CN, and CD_3COCD_3), a situation of rapid exchange between complexed and uncomplexed species is observed on the ^{1}H NMR timescale at 300 MHz: the signals for both host and guest appear as sharp resonances (Fig. 8).[39] Some of the signals—particularly those of the protons on the *n*-butyl chains of **1**-H$^+$ and the γ-OCH_2 resonance of **DB24C8**—are displaced significantly[40] from their original chemical shifts in the absence of the complementary molecule. In $CDCl_3$, the measurement of a stability constant for the [**DB24C8**·**1**-H][PF_6] complex is hampered by the insolubility of the dialkylammonium salt in the absence of a molar equivalent or more of the crown ether. This practical difficulty makes some common techniques for determining K_a values[41]—such as titration or Job's method of continuous variation,[41a] which require spectra to be obtained from solutions that contain less than one equivalent of the host (**DB24C8**)—impossible to use

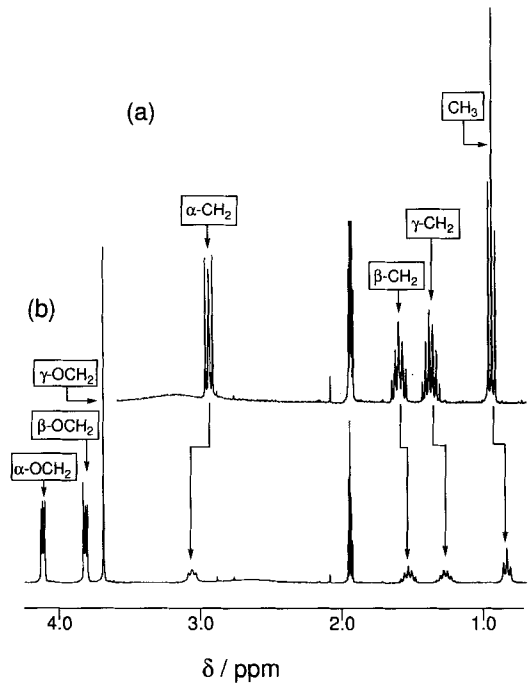

Fig. 8. Partial ^{1}H NMR spectra recorded in CD_3CN at 300 MHz of a) **1**-H·PF_6 and b) a 1:1 mixture of **1**-H·PF_6 and **DB24C8** (ca. 1.0×10^{-3} M).

in this solvent. Although the dilution method[41c,d] is a possible technique for use in chlorinated solvents, dilution of a 1:1 mixture of **1**-H·PF_6 and **DB24C8** in $CDCl_3$ over a range of concentrations did not have a significant effect on the chemical shifts of any of the protons of either host or guest. From this observation, we may conclude that the association constant in $CDCl_3$ is at least of the order of 10^4 L mol^{-1}. In solvents in which both host and guest are individually soluble, we can use standard techniques to determine K_a values.[41] In CD_3CN, the titration method—in which the guest concentration is kept constant whilst the host concentration is varied, or vice versa—led to an estimate of K_a of approximately 50 L mol^{-1}. The dilution experiment, in which the ^{1}H NMR spectra of the 1:1 mixture of **1**-H·PF_6 and **DB24C8** were recorded over a range of concentrations from 5×10^{-2} to 1×10^{-4} M in CD_3CN, gave a value for K_a of approximately 70 L mol^{-1}.

In order to determine an activation barrier for the complexation process, we prepared a solution with a 2:1 molar ratio of **DB24C8** and **1**-H·PF_6 in CD_2Cl_2 and studied the behavior of this mixture by variable-temperature ^{1}H NMR spectroscopy (VTNMR). At room temperature, the spectrum obtained displayed the expected time-averaged sets of signals (Fig. 9). When the sample was cooled down to 0 °C, a gradual broadening of the signals of the crown ether α- and γ-OCH_2 protons occurred, which led eventually, on further cooling, to a separation of both of these signals into two resonances of equal intensity. These two sets of signals are associated with the resonances for the OCH_2 protons in 1) the free **DB24C8** macrocycle and 2) the macrocycle complexed with the dialkylammonium ion to afford a complex, the stoichiometry of which is readily deduced as 1:1 from integration of the signals associated with appropriate probe protons. From the coalescence temperatures of these two probes (−3 °C with a limiting chemical shift difference $\Delta\nu$ at low temperature of 24 Hz for the α-OCH_2 protons, and −7 °C with $\Delta\nu$ = 20 Hz for the γ-OCH_2 protons), the activation barrier ($\Delta G_c^{\ddagger}$) for the process of a dialkylammonium ion exchanging between two **DB24C8** molecules was calculated[42] to be ap-

0947-6539/96/0206-0712 $ 15.00+.25/0 Chem. Eur. J. 1996, 2, No. 6

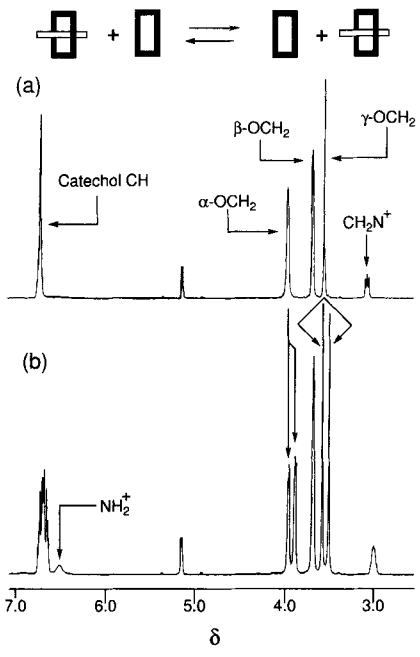

Fig. 9. The ^{1}H NMR spectrum recorded at 400 MHz in CD_2Cl_2 of a solution of **DB24C8** and **1**-H·PF_6 in a 2:1 molar ratio at a) + 30 °C and b) − 27 °C. The spectrum recorded at the higher temperature (a) shows a time-averaged set of signals for both **DB24C8** and **1**-H$^+$. In the spectrum recorded at the lower temperature (b), signals associated with one equivalent of complexed and one equivalent of uncomplexed **DB24C8** are evident for both the α-OCH_2 and γ-OCH_2 protons. The concentrations of the crown ether and the salt are 2.4×10^{-2} and 1.2×10^{-2} M, respectively.

proximately 13.5 kcal mol^{-1}. The chemical shifts of the resonances associated with the *n*-butyl groups of **1**-H·PF_6 are not altered to any great extent over the range +30 to −30 °C. This indicates that the dialkylammonium ion is complexed almost totally at and below room temperature and suggests K_a values of at least 10^4 L mol^{-1} in CD_2Cl_2.

2. *N*,*N*-Dibenzylammonium Hexafluorophosphate (2-H·PF_6) and Dibenzo[24]Crown-8 (DB24C8): As in the case of **1**-H·PF_6, **2**-H·PF_6 is quite insoluble in $CHCl_3$ and CH_2Cl_2—although soluble in more polar solvents. Yet it becomes soluble in these chlorinated solvents in the presence of a molar equivalent or more of the crown ether **DB24C8**. This observation alone is good evidence for the formation of a complex with pseudorotaxane-like geometry. The ^{1}H NMR spectra of a 1:1 mixture of **2**-H·PF_6 and **DB24C8** in a number of different solvents shows an interesting phenomenon—signals associated with the free host and guest are present in the spectrum, as well as those attributable to the 1:1 complex (Fig. 10).[43] This situation arises because of the slow rate of association and dissociation of the complex on the ^{1}H NMR timescale at 300 or 400 MHz at room temperature. Although the *n*-butyl groups of the **1**-H$^+$ ion have little difficulty in threading through **DB24C8**, the relatively bulkier phenyl rings of the **2**-H$^+$ ion do not enjoy the same freedom. The difference between the two systems can be appreciated from inspection of CPK space-filling molecular models of **DB24C8** and **1**- and **2**-H·PF_6. This exercise suggests that a particularly open cavity is required in the crown ether in order to provide a suitable passage for the threading of the benzyl group. Thus, taken together with the fast exchange situation that prevails for the [**DB24C8**·**1**-H][PF_6] complex in solution, this ^{1}H NMR spectroscopic evidence suggested immediately to us that **2**-H·PF_6 forms a complex with **DB24C8** that has a pseudorotaxane-like geometry in solution.

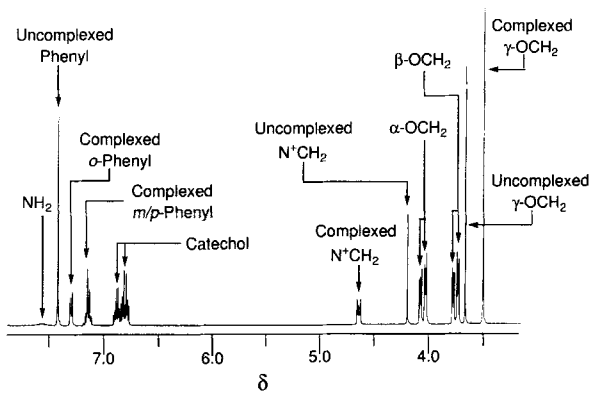

Fig. 10. The ^{1}H NMR spectrum recorded at 400 MHz in CD_3CN of an equimolar mixture of **DB24C8** and **2**-H·PF_6 at 20 °C. The concentrations of both the crown ether and the salt are 1.0×10^{-3} M. Three sets of resonances are evident in this spectrum: 1) for the uncomplexed crown ether, 2) for the uncomplexed salt, and 3) for the 1:1 complex between **DB24C8** and **2**-H·PF_6.

Crystals were grown of this complex and analyzed by FAB mass spectrometry. The mass spectrum shows (Fig. 11) the 1:1 complex without its counterion as the *base peak* (*m*/*z* 646). The uncomplexed dibenzylammonium ion (*m*/*z* 198) gives a substantially weaker signal (ca. 50% of the base peak). The intensity of

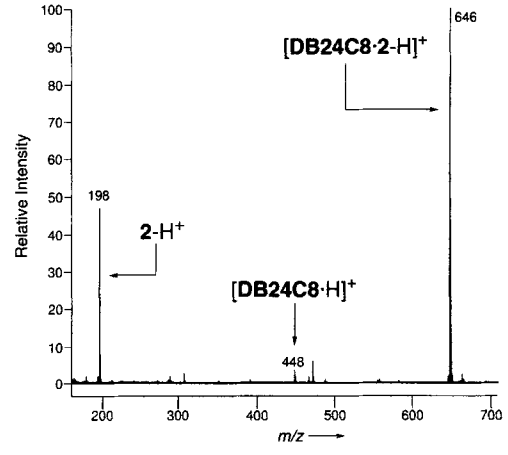

Fig. 11. The FAB mass spectrum of crystals grown of the complex between **DB24C8** and **2**-H·PF_6.

the signal for the 1:1 complex confirms that the association constant between the **2**-H$^+$ ions and **DB24C8** is high and, additionally, that there is a relatively high activation barrier for dissociation of the two species in the "gas phase". Thus, FAB mass spectrometry confirms what we have observed for the [**DB24C8**·**1**-H][PF_6] and [**DB24C8**·**2**-H][PF_6] complexes in solution by ^{1}H NMR spectroscopy—both complexes are quite strong, but the relative rates of association and dissociation of the two complexes are fast and slow, respectively, on the ^{1}H NMR timescale at both 300 and 400 MHz.

The structure of the [**DB24C8**·**2**-H]$^+$ complex was solved by X-ray crystallography on suitable single crystals. Again, a pseudorotaxane-like geometry is adopted. However, the crystal structure differs from that of the [**DB24C8**·**1**-H]$^+$ complex in a number of respects. The complex crystallized (Fig. 12) with two independent 1:1 complexes (**A** and **B**) in the unit cell. In both **A** and **B**, the **DB24C8** molecule adopts conformations (namely, extended all-*gauche* conformations in the polyether chains) that are quite similar to that found for the macrocycle in the

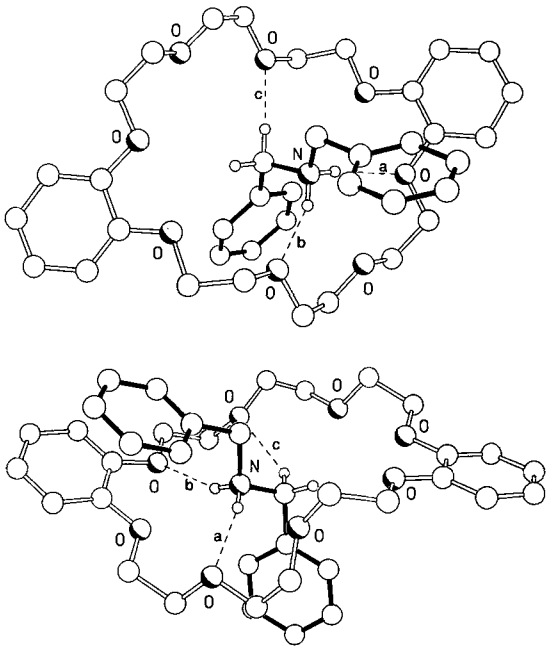

Fig. 12. The superstructures of the 1:1 complexes **A** (top) and **B** (bottom) of [**DB24C8**·**2**-H]$^+$ in the solid state. In **A**, the hydrogen bonds have the following distances and angles: a) [N···O] 3.12 Å, [H···O] 2.24 Å, [N–H···O] 167°; b) [N···O] 2.85 Å, [H···O] 1.99 Å, [N–H···O] 159°; c) [C···O] 3.16 Å, [H···O] 2.21 Å, [C–H···O] 174°. In **B**, the hydrogen bonds have the following distances and angles: a) [N···O] 2.99 Å, [H···O] 2.14 Å, [N–H···O] 157°; b) [N···O] 3.12 Å, [H···O] 2.28 Å, [N–H···O] 155°; c) [C···O] 3.27 Å, [H···O] 2.45 Å, [C–H···O] 143°.

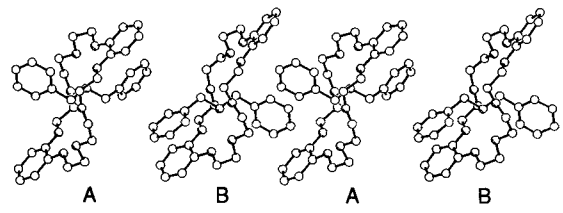

Fig. 13. A portion of the lattice which extends in the crystallographic *c* direction of the [**DB24C8**·**2**-H]$^+$ complex. The complexes stack in the sequence **ABAB** in such a way that the crown-ether components are aligned to form channels though which the ammonium ions are threaded. The stack is, in part, stabilized by a $\pi-\pi$ stacking interaction between phenyl groups in the central complexes (mean interplanar separation, 3.50 Å; centroid–centroid distance, 3.73 Å). The distances between adjacent ammonium ion centers in this stack are 9.3 and 9.7 Å.

[**DB24C8**·**1**-H]$^+$ complex. The manner in which the complexes **A** and **B** differ is in the conformations of the **2**-H$^+$ ions and in the oxygen atoms used in the hydrogen bonding. The cation in **A** adopts a "gull-wing" conformation with the planes of the phenyl rings almost orthogonal to the plane of the all-*anti* C-CH_2-NH_2^+-CH_2-C backbone. In **B**, one of the phenyl rings is inclined by approximately 52° from this plane, whilst the other one is effectively orthogonal. In **A** and **B**, the NH_2^+ center and one of the adjacent CH_2 groups are situated more or less within the plane of their **DB24C8** hosts. In addition, both complexes are stabilized predominantly by two [N–H···O] and one [N–C–H···O] hydrogen bonds between hydrogen atoms of the dialkylammonium NH_2^+ center and one of the adjacent benzylic CH_2 groups, respectively, and polyether oxygen atoms. The oxygen atoms involved in the [N–H···O] hydrogen-bonding interactions of **A** are a phenolic and an aliphatic ether oxygen atom of the same polyether loop, whereas the [N–C–H···O] hydrogen bond utilizes an aliphatic ether oxygen atom on the other loop. In **B**, the hydrogen-bonding motif resembles that found in the [**DB24C8**·**1**-H]$^+$ crystal structure in that the [N–H···O] hydrogen bonds straddle a catechol unit, but the shortest [N–C–H···O] hydrogen-bonding contact is, in this case, with a different oxygen atom. In complex **B**, there is an additional stabilizing interaction as a result of $\pi-\pi$ overlap[44] between one of the phenyl rings of the **2**-H$^+$ ion and one of the catechol units of the crown ether (mean plane separation, 3.48 Å; centroid–centroid distance, 3.79 Å; ring plane/ring plane inclination, 11°). The complexes **A** and **B** pack to form a lattice in the crystallographic *c* direction which repeats in the sequence **A**·**B**·**A**·**B** (Fig. 13). The centrally located phenyl groups are aligned parallel to each other with a mean interplanar separation of 3.50 Å; this arrangement suggests that it is predominantly $\pi-\pi$ stacking interactions that stabilize the lattice. The macrocyclic components of the lattice are aligned such that channels are formed, suggesting the potential of polyrotaxane[45] formation with dialkylammonium-based[46] polymers (Fig. 14).

It may be recalled that a 1:1 mixture of host and guest provides a ^{1}H NMR spectrum that displays the resonances of the complex itself, rather than that of a time-averaged set of resonances between bound and free states (see Fig. 10). This situation provides a rare opportunity to investigate the geometry of the complex directly by NMR spectroscopic methods. In a series of NOE experiments, the signals associated with the resonances of the protons of the 1:1 complex in $CDCl_3$ were irradiated separately and the effect on the resonances associated with the other protons in the system was observed. The results are summarized in Table 1. As an example, irradiation of the signal corresponding to the resonance of the crown ether β-OCH_2 protons resulted in the difference spectrum of Figure 15. In this spectrum, we observe—in addition to enhancements of, and saturation transfer to, complexed and uncomplexed crown ether signals—small, but significant, enhancements of the signal for the benzylic methylene protons and the *o*-protons, and to a lesser extent, for the *m*/*p*-protons on the phenyl ring of the **2**-H$^+$ ion. No NOE enhancement is observed in the resonance for the NH_2^+ protons. Similarly, irradiation of the protons of the γ-OCH_2 group of **DB24C8** led to an enhancement of these same resonances. When the resonance for the α-OCH_2 group was irradiated, the only signal to be enhanced in the **2**-H$^+$ ion were those of the *o*-phenyl protons. Conversely, irradiation of the resonances for the *o* and *m*/*p*-phenyl protons of the **2**-H$^+$ ion led to an enhancement of all three OCH_2 signals for the crown, but irradiation of the signal for the benzylic methylene protons enhanced only the β- and γ-OCH_2 proton resonances. Irradiation of the signals for the catechol protons of **DB24C8** resulted in no observable effect on the resonances of the **2**-H$^+$ ion. The results of this NOE study were consistent with the complex adopting similar geometries (i.e., pseudorotaxane-like) in solution and in the solid state.

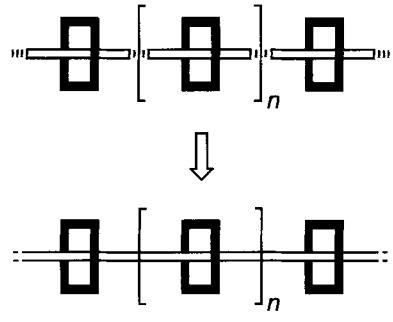

Fig. 14. A cartoon representation of the conceptual progression from a channel of threaded ammonium ions to a polyrotaxane based on a polymer containing secondary dialkylammonium centers.

0947-6539/96/0206-0714 $ 15.00+.25/0 Chem. Eur. J. 1996, 2, No. 6

Table 1. The effects on other protons in the spectrum of a 1:1 mixture of **DB24C8** and **2**-H·PF_6 in $CDCl_3$ upon irradiation of signals of the 1:1 complex [**DB24C8**·**2**-H][PF_6] [a].

Irradiated proton	Observed Signal [b]														
	α-OCH_2 compl.	α-OCH_2 uncompl.	β-OCH_2 compl.	β-OCH_2 uncompl.	γ-OCH_2 compl.	γ-OCH_2 uncompl.	Catechol O-C-C*H*	Catechol O-C-CH-C*H*	Ph-CH_2 compl.	Ph-CH_2 uncompl.	*o*-C_6H_5 compl.	*o*-C_6H_5 uncompl.	*m*/*p*-C_6H_5 compl.	*m*/*p*-C_6H_5 uncompl.	NH_2
α-OCH_2		–	strong NOE	weak NOE/ST	NOE	–	strong NOE	NOE	–	–	NOE	NOE/ST	weak NOE	–	–
β-OCH_2	NOE	NOE/ST		ST	NOE	NOE/ST	NOE	weak NOE	NOE	–	NOE	weak NOE/ST	weak NOE/ST	–	–
γ-OCH_2	NOE	–	NOE	–		ST	–	–	NOE	–	NOE	weak NOE/ST	weak NOE	–	–
catechol O-C-C*H*	NOE	weak NOE/ST	–	–	–	–		strong NOE	–	–	–	–	–	–	–
catechol O-C-CH-C*H*	NOE	weak NOE/ST	–	–	–	–	strong NOE		–	–	–	–	–	–	–
Ph-CH_2	–	–	weak NOE	–	weak NOE	–	–	–		ST	strong NOE	weak NOE/ST	NOE	weak NOE/ST	NOE
o-C_6H_5	weak NOE	–	weak NOE	–	weak NOE	–	–	–	NOE	weak NOE/ST		ST	NOE	weak NOE/ST	NOE
m/*p*-C_6H_5	weak NOE	–	weak NOE	–	weak NOE	–	weak NOE	weak NOE	weak NOE	–	NOE	weak NOE/ST		ST	NOE
NH_2	weak NOE	–	weak NOE	–	weak NOE	–	–	–	NOE	weak NOE/ST	–	–	–	–	

[a] The signals associated with the resonances of each of the protons of the 1:1 complex were irradiated in turn and a difference spectrum obtained. This Table lists the effects observed for all of the other resonances observed in the spectrum. These experiments were performed at 25 °C in $CDCl_3$ (ca. 5.0×10^{-3} M) at 400 MHz. [b] "NOE" (weak or strong) indicates that the relevant signal was enhanced upon irradiation of the probe proton; "ST" refers to a transfer of saturation from the complexed state to the uncomplexed state; "NOE/ST" refers to an NOE enhancement of an uncomplexed probe proton—a result of NOE enhancement of a complexed probe followed by saturation transfer from the complexed to the uncomplexed states.

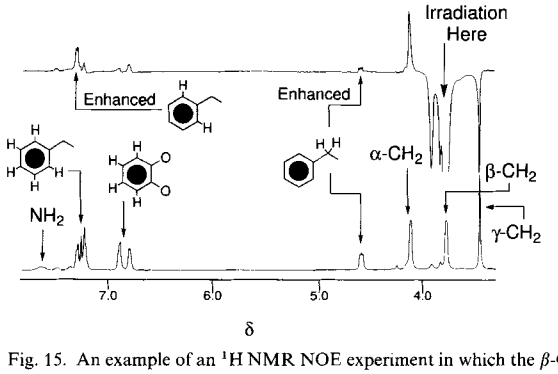

Fig. 15. An example of an ^{1}H NMR NOE experiment in which the β-OCH_2 group of **DB24C8**, complexed with dibenzylammonium hexafluorophosphate (**2**-H·PF_6), is irradiated. The lower spectrum shows the 1:1 mixture in $CDCl_3$—the larger signals correspond to the 1:1 complex and some of the smaller resonances correspond to both uncomplexed components, which are also present. The top spectrum is a difference spectrum. It shows clearly enhancements of the signals for the benzylic methylene protons and the *o*-protons on the phenyl rings of the $\mathbf{2}^+$ cation.

Table 2. Effect of solvent on the association constants (K_a) for the 1:1 complex formed between **DB24C8** and **2**-H·PF_6 in a range of different solvents at 25 °C.

Solvent	ε_r	Gutmann	K_a/L mol^{-1}	$\Delta G°$/ kcal mol^{-1}
	[a]	donor no. [a]	[b]	[c]
CD_3SOCD_3	46.5	29.8	0	–
CD_3COCD_3	20.6	17.0	360	−3.5
CD_3CN	35.9	14.1	420	−3.6
$CDCl_3/CD_3CN$ (1:1)	–	–	1700	−4.4
$CDCl_3$	4.8	4.0	27000	−6.0

[a] Values of the solvent dielectric constants (ε_r) and Gutmann donor numbers were obtained from refs. [5] and [48]. [b] Association constants (K_a) were obtained from "single-point" measurements of the concentrations of the complexed and uncomplexed species in the relevant ^{1}H NMR spectra at 25 °C and using the expression, K_a = [**DB24C8**·**2**-H·PF_6]/[**DB24C8**][**2**-H·PF_6]. [c] The free energies of complexation ($\Delta G°$) were calculated from the K_a values, using the equation $\Delta G° = -RT\ln K_a$.

The observation of signals for the resonances of protons in the 1:1 complex as well as those for free **2**-H·PF_6 and free **DB24C8** in the ^{1}H NMR spectrum of [**DB24C8**·**2**-H][PF_6] provides a convenient single-point method for the measurement[47] of the association constants (K_a) in a number of solvents, since the absolute concentrations of these three species are readily determined from the known total concentrations of host and guest and the calculated relative abundances of the three species. In this manner, we determined K_a values for the [**DB24C8**·**2**-H][PF_6] association in a number of different solvents (Table 2). It is most convenient to compare the K_a values with the Gutmann donor numbers[48] of the various solvents—a clear trend is the increase in association constant with decreasing donor number. For example, in $CDCl_3$—a weak hydrogen bond accepting solvent—the K_a value is highest, whereas, in a solvent with a high donor number, such as CD_3SOCD_3, no complex could be observed at all. It is interesting to compare the K_a values of the complexes of **1**-H·PF_6 and **2**-H·PF_6 with **DB24C8** in the same solvents—they are both of the order of 10^4 L mol^{-1} in $CDCl_3$, and 10^2 L mol^{-1} in CD_3CN. The K_a value in CD_3CN is about five times higher for the [**DB24C8**·**2**-H][PF_6] complex than it is for the [**DB24C8**·**1**-H][PF_6] complex, possibly as a result of 1) the enhanced acidity of the benzylic

methylene protons involved in hydrogen bonding, 2) the presence of additional stabilizing $\pi-\pi$ interactions, or 3) the enhanced binding resulting from better preorganization[2d,e] of the much less flexible **2**-H$^+$ ion.

We have also attempted to observe coalescence of the resonances for the crown ether protons in a 2:1 mixture of **DB24C8** and **2**-H·PF_6 in CD_2ClCD_2Cl in order to determine an activation energy barrier for the association process. However, in this case, heating the ^{1}H NMR sample results only in decomplexation of the pseudorotaxane, and so, rather than observe coalescence behavior, the signals associated with the complexed crown ether diminish in size relative to those of the uncomplexed crown ether signals.

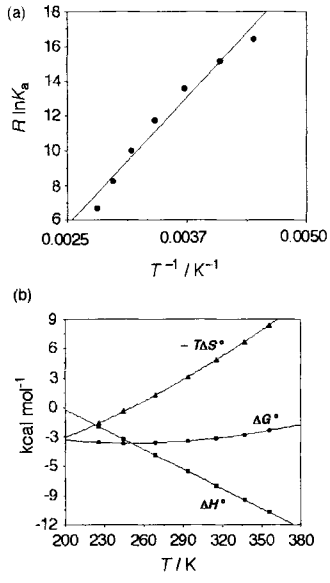

Fig. 16. a) The van't Hoff plot obtained for the association of **2**-H·PF_6 and **DB24C8** in CD_3CN. The plot is clearly nonlinear—with errors in $R\ln K_a$ determination estimated at ± 0.2 kcal mol^{-1}—suggesting significant heat-capacity effects are present. It can be fitted to the modified van't Hoff equation [Eq. (1)]. b) The enthalpic ($\Delta H°$) and entropic ($-T\Delta S°$) contributions of the free energy of association ($\Delta G°$) between **2**-H·PF_6 and **DB24C8** in CD_3CN as calculated with Equation (1). An enthalpy–entropy compensation effect is obviously responsible for maintaining $\Delta G°$ approximately constant over the temperature range.

In order to evaluate the enthalpic ($\Delta H°$) and entropic ($-T\Delta S°$) contributions to the free energy of complexation ($\Delta G°$), we determined the K_a values for the association of **2**-H·PF_6 with **DB24C8** in CD_3CN over a temperature range from -48 to $+83$ °C. For an association process that has temperature-independent enthalpic and entropic components, the van't Hoff plot ($R\ln K_a$ vs. T^{-1}) should result in a straight line with a slope of $-\Delta H°$ and an intercept of $+\Delta S°$.[49] However, the data we obtained when plotted on these axes differs markedly from a straight line (Fig. 16a); this suggests the thermodynamics of complexation are affected[50] by a nonnegligible heat capacity ($\Delta C_p°$). A number of research groups have indicated recently the importance of including a heat capacity term in the van't Hoff equation in this kind of thermodynamical treatment.[51] Dougherty and co-workers have adjusted the equation to take into account such a contribution [Eq. (1)].[51a]

$$R\ln K_a = -(\Delta H_0/T) + \Delta C_p° \ln T + (\Delta S_0 - \Delta C_p°) \quad (1)$$

where
$$\Delta G° = \Delta H° - T\Delta S°$$
$$\Delta H° = \Delta H_0 + T\Delta C_p°$$
$$\Delta S° = \Delta S_0 + \Delta C_p° \ln T$$

We have found that our data fit this modified equation very well and allows us to determine the $\Delta H°$ and $-T\Delta S°$ components of the free energy of complexation of **2**-H·PF_6 and **DB24C8** over the complete temperature range (Fig. 16b). We note the $\Delta H°$ term changes dramatically, such that the enthalpic contribution to $\Delta G°$ decreases with increasing temperature, as the contribution to $\Delta G°$ of $-T\Delta S°$ increases. The curved van't Hoff plots suggest that we should not view this host–guest association as a simple coming together of the complementary species, but rather as a complex series of equilibria involving solvolytic and conformational effects, which are no doubt occurring intermittently between the "free" and "complexed" states.[52]

3. *N,N*-Dibenzylammonium Hexafluorophosphate (2-H·PF_6) and Asym-dibenzo[24]crown-8 (asym-DB24C8): In the first two crystal structures described in this paper so far, it has been noted that, because of the constitution of **DB24C8**, one of the two [N–H···O] hydrogen bonds must involve a phenolic ether oxygen atom of the catechol subunits if the 1,3-alternate oxygen atom sequence preferred by the NH_2^+ center for hydrogen bonding is employed. We reasoned that, if we were to change the position of the catechol units to those found in the isomeric crown ether, asymmetric dibenzo[24]crown-8 (asym-**DB24C8**),[1] then the opportunity for enthalpically favorable hydrogen bonding in the 1,3-alternate arrangement to two *aliphatic* ether oxygen atoms would become available to the dialkylammonium ions. A subtle change in the constitution of the crown ether should otherwise have little effect on its ability to complex with secondary dialkylammonium ions—that is, the cavity of the crown ether should be of a similar size and conformation as **DB24C8** and be suitable for binding $R_2NH_2^+$ ions, at least as deduced from inspection of CPK space-filling molecular models. Although this macrocyclic polyether was first synthesized by Pedersen in 1967,[1] it has rarely been utilized[53] as a host molecule for the binding of cations.

Gratifyingly, a molar equivalent of **2**-H·PF_6—as well as of **1**-H·PF_6—was taken up in a $CHCl_3$ solution of asym-**DB24C8**. ^{1}H NMR Spectroscopy reveals, as expected, a situation involving slow kinetics for complexation and decomplexation of the **2**-H$^+$ ion on the ^{1}H NMR timescale at 400 MHz. Resonances associated with both free and bound host and guest are present in the ^{1}H NMR spectrum (Fig. 17) at room temperature in

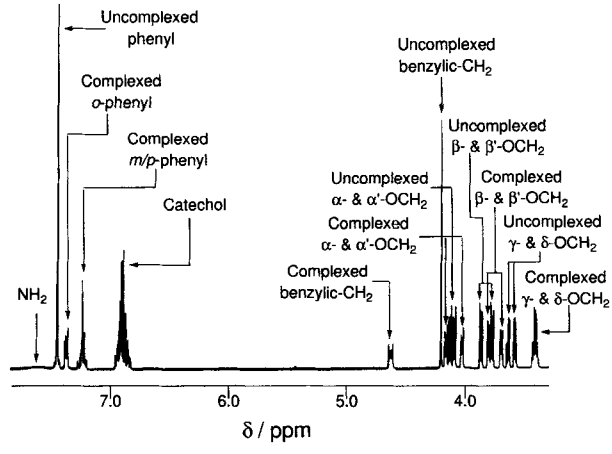

Fig. 17. The ^{1}H NMR spectrum of a 1:1 mixture of asym-**DB24C8** and dibenzylammonium hexafluorophosphate (**2**-H·PF_6) in CD_3CN at 25 °C. A situation of slow kinetic exchange results in signals 1) for uncomplexed asym-**DB24C8**, 2) for uncomplexed **2**-H·PF_6, and 3) for the 1:1 complex formed between the two. The concentration of both host and guest is 1.0×10^{-2} M.

CD_3CN, CD_3COCD_3, and $CDCl_3$. Crystals grown of the complex were analyzed by FAB mass spectrometry. A very strong ion was detected (Fig. 18) in the mass spectrum at m/z 646 for the 1:1 complex after loss of its counterion. Approximately the same proportions of free dibenzylammonium ion **2**-H$^+$ (ca. 90%) and free asym-**DB24C8** (<5%) are present relative to the complex peak, as are present in the FABMS spectrum of the

0947-6539/96/0206-0716 $ 15.00+.25/0 Chem. Eur. J. 1996, 2, No. 6

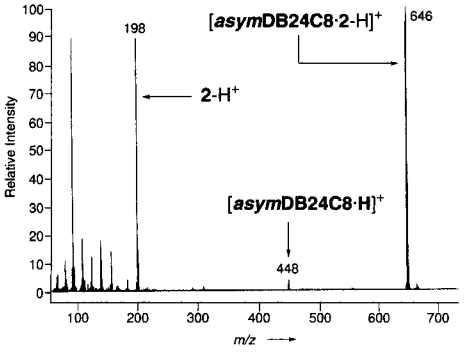

Fig. 18. The FAB mass spectrum of crystals grown of a 1:1 complex between asym-**DB24C8** and dibenzylammonium hexafluorophosphate (**2**-H·PF_6).

[**DB24C8**·**2**-H][PF_6] complex (Fig. 11). These two mass spectra suggest to us that complexation of secondary dialkylammonium ions by either **DB24C8** or asym-**DB24C8** is equally effective.

The X-ray structural analysis of the 1:1 complex formed between the dibenzylammonium cation **2**-H^+ and asym-**DB24C8** (Fig. 19) reveals that the asym-**DB24C8** macrocycle adopts a

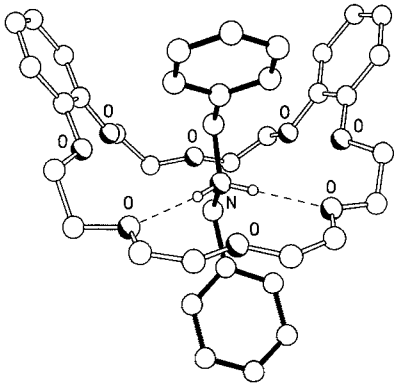

Fig. 19. The solid-state superstructure of [asym-**DB24C8**·**2**-H]$^+$ showing the threading of the dibenzylammonium cation **2**-H^+ through the asym-**DB24C8** macrocycle and the intercomponent [N–H···O] hydrogen bonding. The [N···O] and [H···O] distances and [N–H···O] angles are, respectively, 2.98, 2.94 Å; 2.08, 2.06 Å; and 179, 165°.

horseshoelike conformation with the centroids of the two catechol rings separated by 8.30 Å. Although the shorter polyether chain has a *gauche* conformation for the O-C-C-O units, the central -$OCH_2CH_2OCH_2CH_2O$- portion of the longer chain is approximately planar and exhibits *syn* geometries for its O-C-C-O units. The cation, which adopts a "gull-wing" conformation with the two benzyl rings essentially orthogonal (85 and 86°) to the C-CH_2-NH_2^+-CH_2-C backbone, is threaded through the asym-**DB24C8** cavity with the two phenyl rings folded almost symmetrically over the longer polyether chain. The 1:1 complex is stabilized by a pair of [N–H···O] hydrogen bonds to the second and fourth oxygen atoms of the longer polyether chain. This mode of complexation precludes any secondary intracomplex aryl–aryl interactions between the catechol rings and benzyl groups. However, an inspection of the packing of the 1:1 complexes reveals the formation of a particularly elegant aggregation wherein pairs of 1:1 complexes are arranged such that one of the terminal benzylic phenyl rings of one cation enters into a pair of [C–H···π] interactions (involving both *meta*-CH groups) with both catechol rings of a centrosymmetrically related complex, and vice versa. Simultaneously, the two symmetrically related benzyl groups enter into a parallel face-to-face π–π stacking interaction (Fig. 20). The edge-to-face [C–H···π] interactions have ring centroid/ring centroid separations of 4.89 and 5.00 Å, and the associated [C–H···π] geometries are [H···π] distances of 2.66 and 2.75 Å, with [C–H···π] angles of 159 and 161°, respectively. These [H···π] distances are significantly shorter than those we have observed as part of the stabilizing interactions (ca. 2.85 to 2.95 Å) between hydroquinone

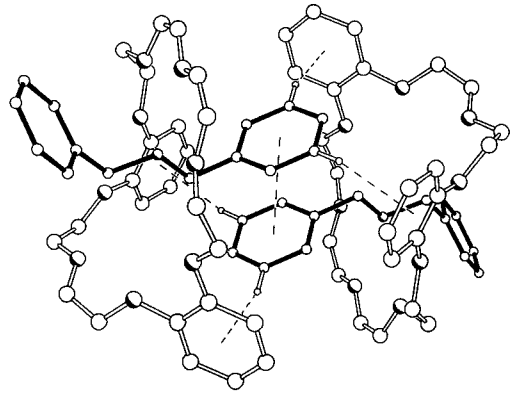

Fig. 20. The cooperative edge-to-face [C–H···π] and face-to-face π–π interactions between pairs of 1:1 complexes in the solid-state superstructure of [asym-**DB24C8**·**2**-H]$^+$.

CH groups and *p*-xylyl rings in a range of [2]catenane structures.[36] The interplanar separation between the two parallelly aligned benzyl groups is 3.44 Å with a centroid/centroid separation of 3.65 Å. Pairs of these complex "dimers" are loosely linked across an independent crystallographic symmetry center through pairs of [C–H···π] interactions involving one of the phenoxymethylene C–H groups in one asym-**DB24C8** of one "dimer" and the catechol ring of another, and vice versa (Fig. 21).

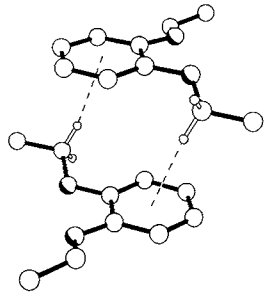

Fig. 21. The secondary inter-"dimer" [C–H···π] interactions in the solid-state superstructure of [asym-**DB24C8**·**2**-H]$^+$. The [H···π] distances and [C–H···π] angles are 2.87 Å and 153°, respectively; the catechol–catechol ring centroid–ring centroid separation is 4.67 Å.

The slow exchange properties of the association of **2**-H·PF_6 and asym-**DB24C8** allow a similar investigation, to that described in Section 2 for this salt with **DB24C8**, of the complex in solution by ^{1}H NMR spectroscopy. Table 3 shows the effect of solvent on the K_a values—once again determined by the single-point method—for this complex. In all the solvents studied, the association constants are similar to those obtained for the [**DB24C8**·**2**-H][PF_6] complex (Table 2), although they are consistently slightly lower in magnitude. This trend may suggest that, although the [asym-**DB24C8**·**2**-H][PF_6] complex can adopt the enthalpically more favorable 1,3-alternate hydrogen-bonding arrangement with two aliphatic ether oxygen atoms—as observed in the crystal structure—this favorable arrangement may be more than compensated for by the involvement of at least one less favorable phenolic ether oxygen atom in all the other 1,3-alternate hydrogen bonding motifs, and the consequent decrease in entropy brought about by avoiding such mo-

Table 3. Effect of solvent on the association constants (K_a) for the 1:1 complex formed between asym-**DB24C8** and **2**-H·PF_6 in a range of different solvents at 25 °C.

Solvent	ε_r [a]	Gutmann donor no. [a]	K_a/L mol^{-1} [b]	$\Delta G°$/kcal mol^{-1} [c]
CD_3SOCD_3	46.5	29.8	0	–
CD_3COCD_3	20.6	17.0	310	−3.4
CD_3CN	35.9	14.1	360	−3.5
$CDCl_3$	4.81	4.0	22000	−5.9

[a] Values of the solvent dielectric constants (ε_r) and Gutmann donor numbers were obtained from refs. [5] and [48]. [b] Association constants (K_a) were obtained from "single-point" measurements of the concentrations of the complexed and uncomplexed species in the relevant ^{1}H NMR spectra at 25 °C and using the expression, K_a = [asym-**DB24C8**·**2**-H·PF_6]/[asym-**DB24C8**][**2**-H·PF_6]. [c] The free energies of complexation ($\Delta G°$) were calculated from the K_a values, using the equation $\Delta G° = -RT\ln K_a$.

tifs. We also examined the temperature dependence on the association constant for the [asym-**DB24C8**·**2**-H][PF_6] complex, since the K_a values are readily obtained by single-point determinations, in CD_3CN. Once again, the resulting van't Hoff plot (Fig. 22a) shows an obvious nonlinearity, and an analysis by means of Equation (1) provided values for $\Delta H°$ and $-T\Delta S°$ over the temperature range from −48 to +85 °C (Fig. 22b). It is interesting to note that the association constant reaches a maximum value of about 1000 L mol^{-1} at approximately −25 °C. This effect suggests that, as before, a classical van't Hoff-style of association does not characterize this system. By comparison, the K_a values obtained for the [**DB24C8**·**2**-H][PF_6] complex continued to increase up to a maximum of approximately 4000 L mol^{-1} at the lowest temperature studied (−48 °C) in CD_3CN.

The 1:1 complex was analyzed by a series of NOE experiments in which all of the resonances associated with the complex were irradiated in turn. The results are summarized in Table 4. Irradiation of the signals for the crown ether α- and α′-OCH_2 protons, simultaneously, resulted in the enhancement of the resonance for the *ortho* protons of the benzylic groups of **2**-H·PF_6. The signals for the β- and β′-OCH_2 protons, when irradiated, affected positively the intensities of the benzyl group's *o*-CH and CH_2-N proton resonances. When the signals for the γ- and δ-protons of asym-**DB24C8** were irradiated, the *o*-CH, *m*/*p*-CH, and benzylic proton resonances of **2**-H·PF_6 were all enhanced. Conversely, when the *o*-CH, *m*/*p*-CH, and benzylic CH_2N^+ proton resonances were irradiated, all the signals for the OCH_2 methylene group protons of the crown ether were enhanced. Irradiation of the catechol residue's resonances had little effect on any of the resonances of **2**-H·PF_6; conversely, the catechol resonances were not affected by irradiation of any of the complexed dialkylammonium salt's resonances. Saturation transfer, and some NOE enhancements resulting from this effect, were evident in all cases, indicating that, although slow, the dynamic processes of complexation and decomplexation are occurring with significant rates on the ^{1}H NMR timescale at 400 MHz. The fact that the signals for the *o*- and benzylic methylene protons were affected by irradiation of the crown ether's β-, β′-, γ-,

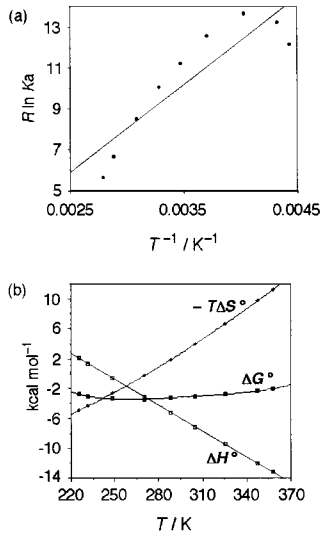

Fig. 22. a) The van't Hoff plot obtained for the association of asym-**DB24C8** and **2**-H·PF_6 in CD_3CN. Again, a significant heat capacity is operative, resulting in the curved set of data points. b) The components of enthalpy ($\Delta H°$) and entropy ($-T\Delta S°$) for the association ($\Delta G°$) between **2**-H·PF_6 and asym-**DB24C8** in CD_3CN as calculated with Equation (1). An enthalpy–entropy compensation effect is obviously responsible for maintaining $\Delta G°$ approximately constant over the temperature range.

Table 4. The effects on other protons in the spectrum of a 1:1 mixture of asym-**DB24C8** and **2**-H·PF_6 in $CDCl_3$ upon irradiation of signals of the 1:1 complex [asym-**DB24C8**·**2**-H][PF_6] [a].

Irradiated proton	Observed signal [b] α/α′-OCH_2 compl.	α/α′-OCH_2 uncompl.	β/β′-OCH_2 compl.	β/β′-OCH_2 uncompl.	γ/δ-OCH_2 compl.	Catechol CH's	Ph-CH_2 compl.	Ph-CH_2 uncompl.	*o*-C_6H_5 compl.	*o*-C_6H_5 uncompl.	*m*,*p*-C_6H_5 compl.	NH_2
α/α′-OCH_2		–	NOE	–	–	NOE	–	–	NOE	NOE/ST	weak NOE	–
β/β′-OCH_2	NOE	–		NOE/ST	NOE	weak NOE	weak NOE	–	NOE	–	weak NOE	–
γ/δ-OCH_2	weak NOE to α-OCH_2	–	NOE to β-OCH_2	–		–	weak NOE	–	NOE	NOE/ST	weak NOE	–
catechol CH's	strong NOE	–	weak NOE	–	–		weak NOE	–	weak NOE	–	weak NOE	–
Ph-CH_2	–	–	weak NOE	–	weak NOE	–		ST	NOE	NOE/ST	–	NOE
o-C_6H_5	weak NOE	–	weak NOE	–	weak NOE	–	NOE	–		ST	NOE	NOE
m/*p*-C_6H_5	weak NOE	–	weak NOE	–	weak NOE	weak NOE	NOE	–	NOE	NOE/ST		NOE

[a] The signals associated with the resonances of each of the protons of the 1:1 complex were irradiated in turn and a difference spectrum obtained. This Table lists the effects observed for all of the other resonances observed in the spectrum. The experiments were performed at 25 °C in $CDCl_3$ (ca. 5.0×10^{-3} M) at 400 MHz. [b] "NOE" (weak or strong) indicates that the relevant signal was enhanced upon irradiation of the probe proton; "ST" refers to a transfer of saturation from the complexed state to the uncomplexed state; "NOE/ST" refers to an NOE enhancement of an uncomplexed probe proton—a result of NOE enhancement of a complexed probe followed by saturation transfer from the complexed to the uncomplexed states.

0947-6539/96/0206-0718 $ 15.00+.25/0 Chem. Eur. J. 1996, 2, No. 6

and δ-OCH_2 protons, and vice versa, is in good agreement with the proposition that the complex has a pseudorotaxane-like geometry in the solution state. These NOE results are very similar to those obtained for the [**DB24C8**·**2**-H][PF_6] complex listed in Table 1—that is, in this previous case, it is also the *o*-CH and benzylic methylene protons that appear to be in close spatial contact with the crown ether OCH_2 protons.

4. *N,N*-Benzyl-*n*-butylammonium Hexafluorophosphate (3-H·PF_6) and Dibenzo[24]Crown-8 (DB24C8): In the case of the first three complexes, we have witnessed the dramatic effects, particularly in the ^{1}H NMR spectra, of varying the substituents on the dialkylammonium ion from a benzyl to an *n*-butyl group—the dibenzylammonium ion **2**-H^+ exhibits slow kinetics of complexation and decomplexation, whereas the di-*n*-butylammonium ion **1**-H^+ undergoes these processes relatively rapidly on the ^{1}H NMR timescale at both 300 and 400 MHz. In these two cases, for different reasons, sharp signals are observed for the protons in both the host and the guest in their ^{1}H NMR spectra. Next, we decided to investigate the effect of introducing asymmetry into the dialkylammonium cations complexed by the crown ethers. We chose a compromise between the two extremes of the **1**-H^+ and **2**-H^+ ions by preparing *N,N*-benzyl-*n*-butylammonium hexafluorophosphate (**3**-H·PF_6). This salt was expected to have kinetics of complexation and decomplexation with **DB24C8** intermediate between those of the two symmetrical ions. Yet again, and perhaps not surprisingly, **3**-H·PF_6 is very close to being insoluble in the chlorinated solvents, $CHCl_3$ and CH_2Cl_2. However, in the presence of one molar equivalent or more of **DB24C8**—and, indeed, of asym-**DB24C8**—solubility of the salt is achieved. The ^{1}H NMR spectrum of a 1:1 mixture of **3**·HPF_6 and **DB24C8** in a number of different solvents shows that the kinetics lie somewhere between those of the complexes with **DB24C8** involving **1**-H·PF_6 and **2**-H·PF_6. At room temperature, the rates of complexation and decomplexation are slow enough to result in broad signals for both the host and guest proton resonances. Analysis of the complex by FAB mass spectrometry reveals (Fig. 23) an intense peak at *m/z* 612 for the 1:1 complex, [**DB24C8**·**3**-H]$^+$. This peak has an intensity of

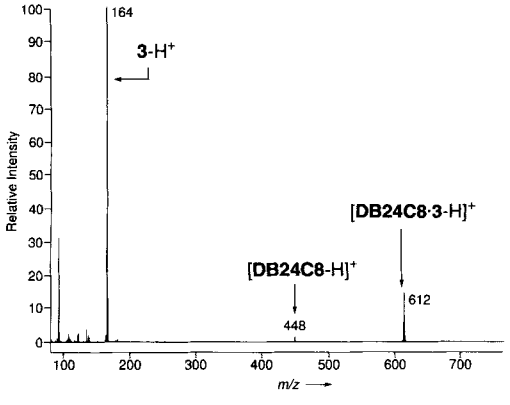

Fig. 23. The FAB mass spectrum obtained for the 1:1 complex between **DB24C8** and benzyl-*n*-butylammonium hexafluorophosphate (**3**-H·PF_6).

approximately 15% of the height of the base peak, which can be assigned to the uncomplexed **3**-H^+ ion; this suggests that dissociation of the [**DB24C8**·**3**-H]$^+$ complex occurs more readily than that of the [**DB24C8**·**2**-H]$^+$ complex. This situation is consistent with an *n*-butyl group unthreading itself from **DB24C8** more readily than a benzyl group.

X-ray crystallography was performed on suitable single crystals, providing a solid-state structure for the complex. [**DB24C8**·**3**-H][PF_6] crystallizes with two crystallographically independent 1:1 complexes (**A** and **B**) with distinctly differing encapsulation geometries. In both cases, the **DB24C8** macrocycle adopts an open "horseshoe" conformation (Fig. 24) with

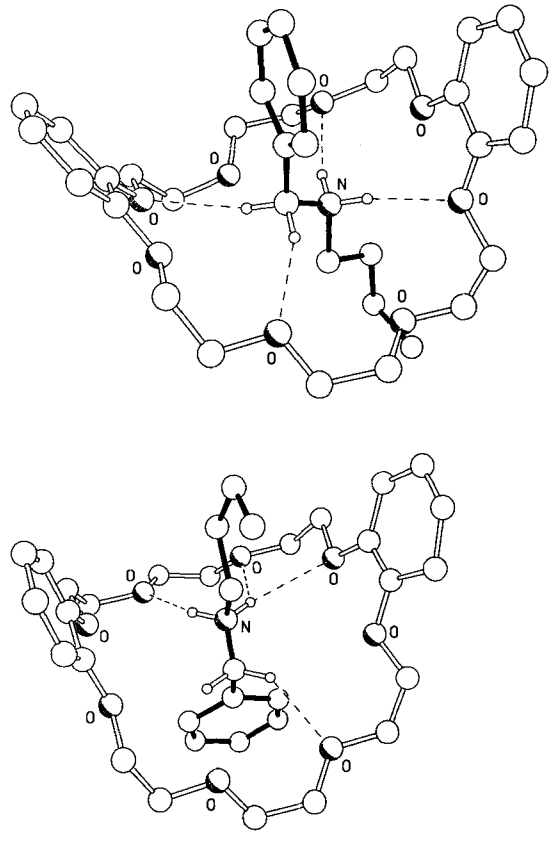

Fig. 24. Ball-and-stick representations of the two crystallographically independent 1:1 complexes, **A** (top) and **B** (bottom), of [**DB24C8**·**3**-H]$^+$ in the solid state. In **A**, the [N–H···O] hydrogen bonds have the following distances and angles: [N···O] 2.99, 3.07 Å; [H···O] 2.11, 2.18 Å; [N–H···O] 167, 170°, respectively; the [C–H···O] hydrogen bonds have the following distances and angles: [C···O] 3.29. 3.36 Å; [H···O] 2.37, 2.43 Å; [C–H···O] 161, 162°, respectively. In **B**, the [N–H···O] hydrogen bonding geometries are [N···O] 3.18, 3.05, 3.02 Å; [H···O] 2.37, 2.36, 2.21 Å; [N–H···O] 150, 134, 150°, respectively. The [C–H···O] hydrogen-bonding geometry is [C···O] 3.16 Å, [H···O] 2.32 Å and [C–H···O] 146°.

the two catechol rings inclined by 49 and 46° in the independent 1:1 complexes **A** and **B**, respectively. There are two distinct threading geometries for the benzyl-*n*-butylammonium cation **3**-H^+. In complex **A**, the benzyl group is sandwiched approximately centrally[54] between the two catechol rings of the host, but with the plane of its phenyl ring approximately parallel to one of the catechol rings (14° tilt), even though the ring centroid/ring centroid separation and mean interplanar separation (4.34 and 3.91 Å, respectively) are too large for any significant π–π stabilization to occur. The principal host–guest stabilization is a result of both [N–H···O] and [C–H···O] hydrogen bonding to pairs of diammetrically disposed aryl and alkyl ether oxygen atoms, with both NH_2^+ hydrogen atoms and both benzylic methylene hydrogen atoms being utilized as donors (Fig. 24, top). In complex **B**, the cation is directed in the opposite direction through the center of the **DB24C8** macrocycle, such that the terminal methyl group on the *n*-butyl substituent is positioned between the two catechol rings (cf. the benzyl group in complex **A**). Host–guest binding involves both hydro-

gen atoms at the NH_2^+ center and one of the benzylic methylene hydrogen atoms in the cation with four polyether oxygen atoms in the crown ether (Fig. 24, bottom). There is a marked absence of any intercomplex [π–π] or [C–H···π] interactions.

A 1:1 mixture of **3**-H·PF_6 and **DB24C8** was studied by VT ^{1}H NMR spectroscopy in $CDCl_3$. At 33 °C, very broad peaks are observed (Fig. 25a) for both the host and guest proton resonances as a result of slow exchange between complexed

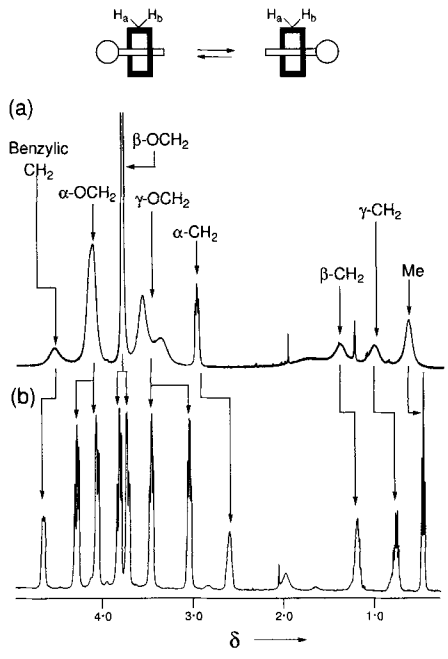

Fig. 25. The partial ^{1}H NMR spectrum at 400 MHz in $CDCl_3$ of a solution of **DB24C8** and **3**-H·PF_6 in a 1:1 molar ratio recorded at a) + 33 °C and b) – 27 °C. The spectrum recorded at the higher temperature (a) shows broad signals associated with both **DB24C8** and **3**-H^+, indicating that an exchange process is occurring at rates approximating to those of the ^{1}H NMR timescale. At the lower temperature (b), the signals associated with the OCH_2 protons on the two heterotopic faces of the crown ether appear as separate sets of resonances.

and uncomplexed states. On warming up the $CDCl_3$ solution, the spectrum simplifies to a situation characteristic of faster exchange. However, the peaks are still quite broad, and a substantial amount of decomplexation undoubtably also occurs, since the chemical shifts of the signals more closely resemble those of the two uncomplexed components. On cooling the sample down to –27 °C (Fig. 25b), however, the signals associated with the three different OCH_2 groups of **DB24C8** separate into two multiplets in each case on account of a very slow rate of decomplexation. The outcome is that heterotopicity characterizes the two faces of the crown ether as a consequence of the constitutional asymmetry of the **3**-H^+ ion: one face of the **DB24C8** ring experiences the shielding influence of the benzyl group, while the chemical shifts of the other face are affected only slightly by the presence of the *n*-butyl chain.[55] Low-intensity signals, which correspond to the resonances of both free **DB24C8** and free **3**-H·PF_6, are also present in the spectrum. By measuring the coalesence temperatures associated with both the α- and β-OCH_2 methylene group resonances, we have obtained an estimate for the activation energy barrier for the process of the **3**-H^+ ion decomplexing from **DB24C8**, reorienting itself, and complexing once again with the crown ether. The $\Delta G^{\neq}$ value was found[42] to be approximately 14.6 kcal mol^{-1} based on the two probe protons (α-OCH_2: T_c = + 36 °C, limiting chemical shift difference ($\Delta\nu$) at low temperature of 86 Hz; β-OCH_2: T_c = +15 °C, $\Delta\nu$ = 35 Hz). These coalescence temperature measurements are rendered difficult by the dissociation of the complex on heating. On approaching the coalescence temperature for the resonances of the various different probe protons, the signals for a significant amount of uncomplexed crown ether interfere with the signals of one or other of the two resonances associated with each OCH_2 group, making the accurate determinations of the coalescence temperatures a difficult task. Coalescence of the signals for the γ-OCH_2 protons was not observed on account of the fact that total dissociation of the complex occurs before the coalescence temperature is reached in the case of this particular probe.

5. *N,N*-Dibenzylammonium Hexafluorophosphate (2-H·PF_6) and Bis(*p*-phenylene)[34]Crown-10 (BPP34C10): So far, we have considered only complexes of macrocyclic polyethers of the [24]crown-8 constitution (**DB24C8**, asym-**DB24C8**) with secondary dialkylammonium ions (**1**-H^+, **2**-H^+, **3**-H^+). We also became interested in studying the behavior of other crown ethers—especially larger ones—toward binding the ions **1**-H^+, **2**-H^+ and **3**-H^+. A crown ether that has been used extensively in the past within our research group is bis(*p*-phenylene)-[34]crown-10 (**BPP34C10**). This macrocyclic polyether has proven to be remarkably effective in the template-directed syntheses of [*n*]rotaxanes[36a, 56] and [*n*]catenanes[36] as a result of its strong association with bipyridinium and related dicationic units in dumbbell-shaped and cyclophane components, respectively. **BPP34C10** was prepared initially by Cram and co-workers[12c] who thought it might be a suitable receptor for binding *two* primary alkylammonium ions (RNH_3^+) simultaneously within its two polyether loops as a result of the presence of two discrete three-point [N–H···O] hydrogen bonding motifs. However, the association constants for the binding of ammonium (NH_4^+) and *tert*-butylammonium (*t*BuNH_3^+) picrates with **BPP34C10** were found to be approximately three orders of magnitude lower than those for the binding of these same cations with **18C6** derivatives. Poor preorganization was suggested by the authors as an explanation for the weaker binding. The question we asked ourselves was what its complexation behavior would be toward secondary dialkylammonium ions ($R_2NH_2^+$) where two-point [N–H···O] hydrogen bonding might be expected to occur.

N,N-Dibenzylammonium hexafluorophosphate (2-H·PF_6) can be dissolved in $CHCl_3$ and CH_2Cl_2 in the presence of an *equimolar* amount of **BPP34C10**. However, the ^{1}H NMR spectrum, obtained after filtration of a suspension of an excess of **2**-H·PF_6 in CD_2Cl_2 containing **BPP34C10**, showed a stoichiometry associated with a 1:2 complex, [**BPP34C10**·(**2**-$H)_2$][PF_6]$_2$ (Fig. 26). The fact that 2 molar equivalents of the salt are taken up into solution suggests that the association constants for the complexes formed are high (ca. 10^3–10^4 L mol^{-1}). The ^{1}H NMR spectrum re-

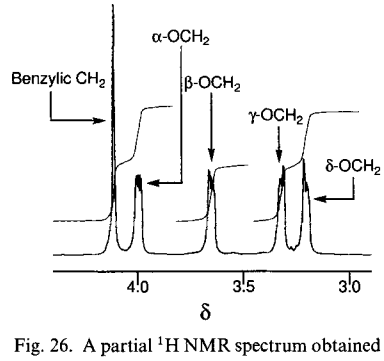

Fig. 26. A partial ^{1}H NMR spectrum obtained in CD_2Cl_2 following extraction of a suspension of dibenzylammonium hexafluorophosphate (**2**-H·PF_6) by **BPP34C10**. A situation of fast kinetic exchange results—by integration of the appropriate signals a stoichiometry for the complex is determined as being 1:2 (host:guest). The association constants for this process are estimated to be of the order of 10^3–10^4 L mol^{-1}.

0947-6539/96/0206-0720 $ 15.00+.25/0

corded at 400 MHz reveals a time-averaged set of signals for both the host and guest, indicating that fast kinetic exchange is occurring between complexed and uncomplexed states. Significant changes are observed[57] in the chemical shifts of the benzylic methylene protons in the **2**-H^+ ion and of the γ- and δ-OCH_2 protons in **BPP34C10** relative to the δ values obtained when they are in their uncomplexed states. Crystals of this complex were subjected to FAB mass spectrometry and gave (Fig. 27) an ion of mass *m/z* of 1077, corresponding to the 1:2 complex having lost *one* of its PF_6^- counterions, as well as a much more intense peak at *m/z* 734 for a complex with 1:1 stoichiometry minus one of its PF_6^- counterions.

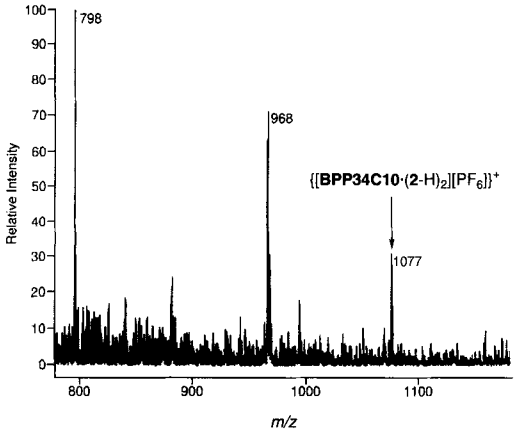

Fig. 27. The FAB mass spectrum obtained from crystals grown of the 1:2 complex between **BPP34C10** and **2**-H·PF_6. The peak of highest mass is that found for a 1:2 complex: this ion has an abundance of less than 1% relative to the base peak, which correponds to the uncomplexed, but protonated, **BPP34C10**.

Single crystals, suitable for X-ray analysis, were grown from an *equimolar* solution of **2**-H·PF_6 and **BPP34C10** in an acetone–pentane mixture of solvents. An intriguing centrosymmetric superstructure characterizes this complex with its 1:2 stoichiometry (Fig. 28). *Two* $\mathbf{2}^+$ ions are threaded through the cavity of **BPP34C10**, and the [N···N] distance is 8.4 Å. The macrocycle adopts an open centrosymmetric geometry with parallelly aligned hydroquinone rings (*syn* geometry) and a centroid/centroid distance of 6.99 Å, similar to that found in one of the two molecules present in the unit cell of the crystal structure[36a] of the free macrocycle. The dialkylammonium ions adopt a conformation quite different from that of the "gull-wing" observed in the [**DB24C8**·**2**-H][PF_6] and [asym-**DB24C8**·**2**-H][PF_6] complexes. In this 1:2 complex, an *anti-gauche* arrangement is favored about the C-N-C bonds. The NH_2^+ centers are located slightly above and below the plane of the macroring, respectively. The complex is stabilized by two [N–H···O] hydrogen bonds in the case of each dibenzylammonium ion. Although bifurcated, the shortest of the NH_2^+ hydrogen bonds are with adjacent aliphatic ether oxygen atoms on the same polyether chain of the macrocycle, that is, a 1,2-adjacent, rather than the more usual 1,3-alternate, hydrogen-bonding motif is observed. There appear to be no [N–C–H···O] hydrogen bonds. Although these types of hydrogen bonds occur in the crystal structures involving the **24C8**-sized macrocycles, because the hydrogen atoms of the NH_2^+–CH_2 groups are surrounded by polyether oxygen atoms, **BPP34C10** cannot participate in this additional hydrogen bonding simply because the *p*-phenylene groups in the crown ether dictate that the two polyether loops are far too distant from each other to sustain [N–C–H···O] hydrogen bonds. Further stability is conferred upon the [**BPP34C10**·(**2**-$H)_2$][PF_6]$_2$ complex, in the absence of [N–C–H···O] hydrogen bonding, by aromatic–aromatic edge-to-face interactions[58] between the π face of a phenyl ring of each **2**-H^+ cation and an *ortho*-hydroquinone hydrogen atom of the crown ether (centroid/centroid separation, 5.06 Å; H···ring centroid distance, 2.73 Å; C–H···centroid angle, 171°). There are no dominant stabilizing interactions between the 1:2 complexes. However, as in the case of the [**DB24C8**·**1**-H][PF_6] and [**DB24C8**·**2**-H][PF_6] solid-state superstructures, the crown ether components in the lattice of the complex [**BPP34C10**·(**2**-$H)_2$][PF_6]$_2$ align themselves so as to form channels in the crystallographic *c* direction (Fig. 29), conjuring up the prospect of doubly threaded polyrotaxanes. In this stack, the distance between the closer of the N^+ centers is 6.9 Å. This 1:2 complex is a rare example of a double-stranded pseudorotaxane. Up until now, superstructures such as these have been found most commonly in the inclusion complexes of γ-cyclodextrins.[59]

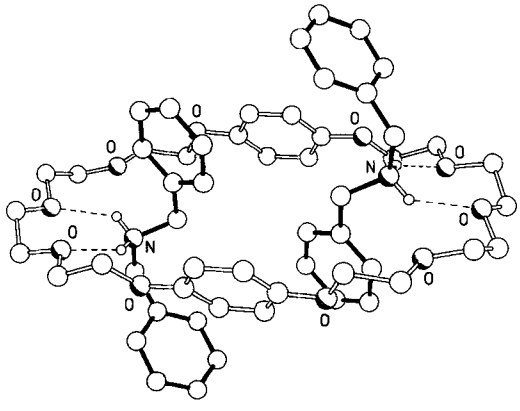

Fig. 28. The superstructure of the 1:2 complex of [**BPP34C10**·(**2**-$H)_2$]$^{2+}$ in the solid state. The [N–H···O] hydrogen bonds have the following distances and angles: [N···O] 2.83, 2.82 Å, [H···O] 2.10, 2.06 Å, [N–H···O] 137, 141°.

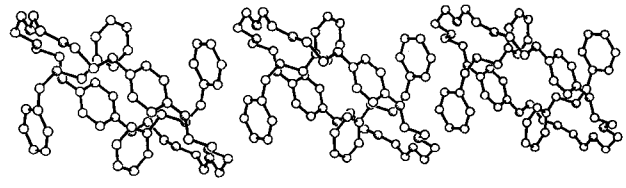

Fig. 29. Ball-and-stick representation showing the pseudopolyrotaxane stacking motif in the crystals of [**BPP34C10**·(**2**-$H)_2$]$^{2+}$.

6. α,α′-Bisbenzylammonium-*p*-xylene Bis(hexafluorophosphate) (4-H_2·$[PF_6]_2$) and Bis(*p*-phenylene)[34]Crown-10 (BPP34C10): All the complexes described so far have relied upon the involvement of secondary dialkylammonium salts bearing one ammonium center (**1**-H·PF_6, **2**-H·PF_6, and **3**-H·PF_6). We have found in some of these complexes in the solid state that channels are formed in which crown ether molecules are aligned in a manner reminiscent of polyrotaxanes. We observed in [**BPP34C10**·(**2**-$H)_2$][PF_6]$_2$ that two dialkylammonium ions may be accommodated within the cavity of **BPP34C10**. The next question was what the effect would be of complexing a bisdialkylammonium salt with this macrocyclic polyether. Would a 1:1 complex be formed in which both NH_2^+ centers are accommodated within the same macrocycle, would two crown ether rings encircle the same threadlike molecule, or would a 2:2 complex be formed between two bisdialkylammonium dications and two crown

ethers? As a first step toward building up oligomeric systems, we prepared α,α′-bisbenzylammonium-*p*-xylene bis(hexafluorophosphate) (**4**-$H_2\cdot[PF_6]_2$) by a simple sequence of reactions from commercially available starting materials.[25]

The bisammonium salt **4**-$H_2\cdot[PF_6]_2$ is soluble in polar organic solvents such as MeCN, Me_2CO, DMSO, and MeOH, but is insoluble in the halogenated solvents, $CHCl_3$ and CH_2Cl_2. Unlike the dialkylammonium salts discussed previously, it is not possible to dissolve **4**-$H_2\cdot[PF_6]_2$ in $CHCl_3$ and CH_2Cl_2 even in the presence of several molar equivalents of **BPP34C10**. The insolubility results possibly from having to solvate two NH_3^+ centers simultaneously, a process which is entropically unfavorable. However, a 1:1 mixture of **BPP34C10** and **4**-$H_2\cdot[PF_6]_2$, when dissolved in CD_3CN, may be diluted with CD_2Cl_2 (3 v/v relative to CD_3CN) such that the ammonium salt remains in solution. In the ^{1}H NMR spectrum, substantial shifts[60] are observed for the benzylic methylene protons and for the aromatic protons associated with the central *p*-xylyl group of the bisdialkylammonium salt, indicating that a complex of some kind is formed in solution. Crystals of the complex were analyzed by FAB mass spectrometry. A peak for a 2:2 complex is not observed in the mass spectrum; rather, a peak at *m/z* 999, which corresponds to a 1:1 complex with the loss of one PF_6^- counterion, is observed.

Single crystals were obtained from a 1:1 mixture of **BPP34C10** and **4**-$H_2\cdot[PF_6]_2$ in an acetone solution when it was layered with pentane. These crystals proved to be suitable for X-ray crystallographic analysis. The superstructure is depicted in Figure 30 and, surprisingly, it is that of a 2:2 complex, obtained from the threading of two dications **4**-H_2^{2+} through two adjacent macrocycles, to give a double-stranded, doubly threaded pseudorotaxane! The 2:2 complex [(**BPP34C10**)$_2\cdot$(**4**-H_2)$_2$]$^{4+}$ is stabilized in the crystal by a series of hydrogen bonds—ten [N–H···O] and four [N–C–H···O] close contacts. All four NH_2^+ center–polyether interactions are different, since the conformations of both macrocycles and both dications are nonequivalent; that is, the complex is totally asymmetric. The macrocycles adopt conformations similar to that observed in the [**BPP34C10**$\cdot$(**2**-H)$_2$]$^{2+}$ complex (e.g., a *syn* geometry is adopted with respect to the hydroquinone units), although the hydroquinone residues are somewhat twisted from the parallel arrangement observed in the 1:2 complex and are inclined by 30 and 26° with ring centroid/ring centroid distances of 7.18 and 7.00 Å, respectively. The conformations of the **4**-H_2^{2+} dications are quite similar and adopt "gull-wing" conformations (all-*anti* C-CH_2-NH_2-CH_2-C backbone) about the NH_2^+ centers, with a *syn* arrangement about the central *p*-xylyl unit (NH_2-CH_2-C_6H_4-CH_2-NH_2). As in the case of the 1:2 complex discussed in Section 5, the [(**BPP34C10**)$_2\cdot$(**4**-H_2)$_2$]$^{4+}$ complex packs with the macrocycles forming a tubular array in the crystallographic *b* direction (Fig. 31).

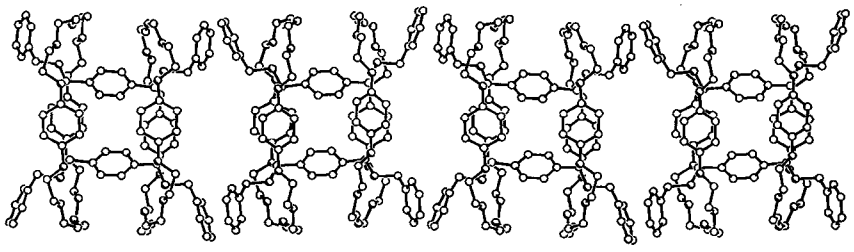

Fig. 31. Part of the lattice of the [(**BPP34C10**)$_2\cdot$(**4**-H_2)$_2$]$^{4+}$ complex, with the channels running from left to right.

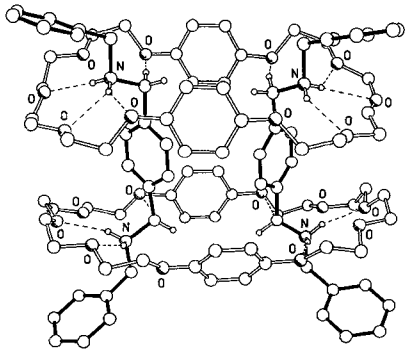

Fig. 30. The superstructure of the 2:2 complex of [(**BPP34C10**)$_2\cdot$(**4**-H_2)$_2$]$^{4+}$ in the solid state. The [N–H···O] hydrogen bonds have the following distances and angles: [N···O] 2.85–3.01 Å, [H···O] 2.02–2.27 Å, [N–H···O] 127–168°. The [C–H···O] hydrogen bonds have the following distances and angles: [C···O] 3.25–3.43 Å, [H···O] 2.32–2.48 Å, [C–H···O] 158–167°.

Does a 2:2 complex exist in the solution and "gas" phases as well? This question is difficult to answer with certainty in the solution state by ^{1}H NMR spectroscopy where we detect a complex with (empirical) 1:1 stoichiometry. In the mass spectrum, we observe a peak for an ion with 1:1 stoichiometry (*m/z* 999). This peak was confirmed to arise from a 1:1 complex—and not a doubly charged 2:2 complex—by the characteristic isotope pattern for this ion, which showed increments of approximately one Dalton between peaks. The remarkable assembly formed in the solid state is a rare example of a double stranded and doubly encircled superstructure, only proposed in the literature previously for inclusion complexes of β- and γ-cyclodextrin.[59] The X-ray crystal structure suggests an intriguing possibility of linking the two termini of each dication with a suitable spacer group to prepare novel [4]catenanes in which each macrocycle is catenated by two other macrocycles (Fig. 32). Another possible development would be the formation of polyrotaxanes, where two independent polymer chains are threaded through the same macrocycle. Thus, the macrocycle could be viewed as a noncovalent cross-linking agent. Since the polymers would be based on polydialkylamines, it might be possible to control polymer gelation by changes in pH.

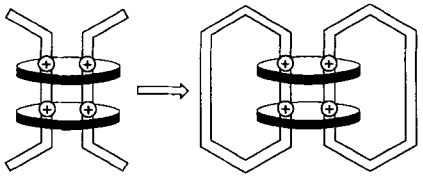

Fig. 32. A cartoon representing the progression conceptually from the double encircled and doubly threaded 2:2 complex, [(**BPP34C10**)$_2\cdot$(**4**-H_2)$_2$]$^{4+}$, to a novel class of [4]catenane in which each macrocycle is catenated by two other macrocycles.

7. α,α′-Bisbenzylammonium-*p*-xylene Bis(hexafluorophosphate) (4-$H_2\cdot[PF_6]_2$) and Dibenzo[24]crown-8 (DB24C8): In the knowledge that the bisammonium salt **4**-$H_2\cdot[PF_6]_2$ leads to a 2:2 complex with **BPP34C10**, we expected this dication to be a suitable candidate to form a 2:1 (host:guest) complex with the smaller crown ether, **DB24C8**. This expectation was justified by

0947-6539/96/0206-0722 $ 15.00+.25/0 Chem. Eur. J. 1996, 2, No. 6

the results we obtained. Although the salt does not dissolve in a $CHCl_3$ solution containing **DB24C8**, once **4**-$H_2\cdot[PF_6]_2$ is dissolved in the minimum amount of CD_3CN, the crown ether can be added as a $CHCl_3$ solution without precipitation of the salt. Indeed, in this manner, a solution containing relatively little CD_3CN may be prepared without precipitation of the complex. This observation indicates that a complex forms—probably with a [3]pseudorotaxane geometry—in what is effectively a $CDCl_3$ solution, with high association constants (ca. $10^4\,L\,mol^{-1}$). The ^1H NMR spectrum of a 2:1 mixture of **DB24C8** and **4**-$H_2\cdot[PF_6]_2$ in CD_3CN is complex. Since the association constants for the equilibria are expected to be of the order of approximately $10^2\,L\,mol^{-1}$, and slow complexation and decomplexation is expected to prevail on the ^1H NMR timescale at 300 MHz as a result of the difficulty of threading a phenyl ring through a 24-membered ring, one might expect that the ^1H NMR spectrum would reveal the presence of free **DB24C8** and free **4**-$H_2\cdot[PF_6]_2$, as well as the 1:1 and 2:1 complexes formed between the two species. These four discrete species are indeed all observed in solution at room temperature in CD_3CN. In order to determine which resonances correspond to the 2:1 complex, the spectrum of **4**-$H_2\cdot[PF_6]_2$ was recorded in a CD_3CN–$CDCl_3$ mixture (1:1 v/v) with a large excess of **DB24C8** (10 mol equiv). Because of the slow kinetics and large association constant in the case of the less polar solvent, a situation arises in which only two major species are observed in solution—the 2:1 complex, [(**DB24C8**)$_2\cdot$**4**-H_2][PF_6]$_2$, and excess of the uncomplexed **DB24C8** (Fig. 33). The signals for the protons of the two different benzylic methylene groups in the **4**-H_2^{2+} dication appear as two multiplets as a result of coupling to the NH_2^+ protons when they are complexed within the macrocyclic polyether. The crown ether resonances are shifted quite substantially from the δ values observed for the protons of the uncomplexed crown ether, and the resonances of the protons on the two faces of the macrocycle (i.e., the OCH_aH_b groups of the polyether chains) are separated into two sets of resonances each, since the two faces of the crown ether are heterotopic in the complex. One face is directed toward the central *p*-xylyl unit and the neighboring crown ether, whereas the other face is directed toward a terminal benzyl group. Thus, heterotopicity is induced in the two faces of the complexed crown ether, in a manner similar to that observed for the 1:1 complex found between **DB24C8** with the benzyl-*n*-butylammonium salt, **3**-H·PF_6, at low temperatures. The stoichiometry of the complex formed between **DB24C8** and the **4**-H_2^{2+} dication is readily determined to be 2:1 (host:guest) by the relative integration of the signals associated with the resonances of both the complexed host and guest.

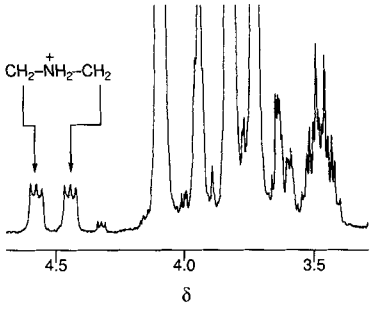

Fig. 33. The partial ^1H NMR spectrum of a 10:1 mixture of **DB24C8** and the bisammonium salt, **4**-$H_2\cdot[PF_6]_2$, in $CD_3CN/CDCl_3$ (1:1, v/v). The excess of crown ether and the use of a solvent mixture which is a poor hydrogen-bond donor results in a situation where two major species exist in solution—the 2:1 complex, [(**DB24C8**)$_2\cdot$**4**-H_2][PF_6]$_2$, and excess of uncomplexed **DB24C8**.

FAB Mass spectrometry on crystals grown of the complex results (Fig. 34) in a peak at *m/z* 1360 corresponding to a 2:1 complex having lost one of its counterions. The base peak at *m/z* 765 in the mass spectrum corresponds to that of a 1:1 complex

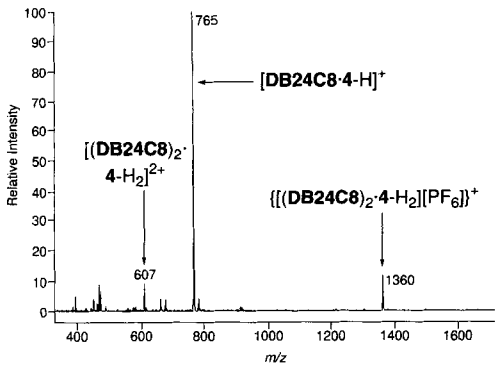

Fig. 34. The FAB mass spectrum of crystals grown of the complex formed between **DB24C8** and **4**-$H_2\cdot[PF_6]_2$. The highest mass peak corresponds to a 2:1 complex with the loss of one counterion—an intense signal for a ternary complex. The base peak in the spectrum corresponds to a 1:1 complex having lost both its counterions. A peak representing the 2:1 complex without any counterions and doubly charged appears at *m/z* 607.

which has lost both of its counterions. The peak for the 2:1 complex has an intensity of approximately 10% of the height of the base peak, indicating that a reasonably strong 2:1 complex exists in the "gas phase", as well as in solution.

The superstructure of the complex was determined by X-ray crystallography on suitable single crystals. Indeed, a 2:1 complex is formed (Fig. 35) in which one bisdialkylammonium dication **4**-H_2^{2+} is encircled by two **DB24C8** macrocycles. The 2:1 complex is centrosymmetric with respect to the central *p*-xylene ring and is stabilized by a total of six [N–H···O] and two [N–C–H···O] hydrogen bonds. The [N–H···O] hydrogen bonds are directed in a 1,3-alternate arrangement at oxygen atoms that straddle catechol units, although they are somewhat bifurcated. In addition to the hydrogen bonds, the complex is stabilized by an almost parallelly alligned π–π stacking motif between the central *p*-xylyl ring and one catechol unit from each macrocycle. These rings are inclined by approximately 5° and have ring centroid/ring centroid separations of 3.65 Å. The 2:1 complexes are associated (Fig. 36) in the crystallographic *a* direction by a [C–H···π] interaction between one of the phenoxymethylene CH groups in one **DB24C8** of a 2:1 complex and the other catechol ring in its lattice-translated counterpart. The [H···π] distance is 2.71 Å and the [C–H···π] angle is 146° There is no sign of channel formation in the lattice. However, we see quite clearly the prospect of pseudopolyrotaxanes *within* the complexes—all that would be required would be a polydialkylammonium threadlike polymer with suitably spaced NH_2^+ centers.

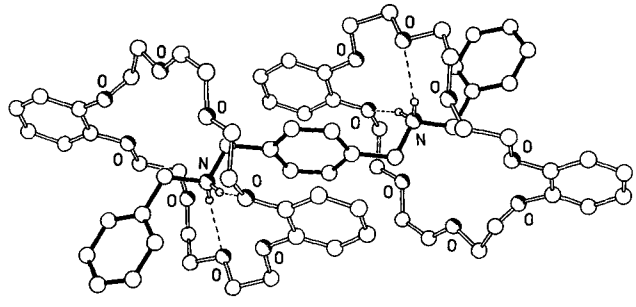

Fig. 35. The superstructure of the 2:1 complex of [(**DB24C8**)$_2\cdot$**4**-H_2]$^{2+}$ in the solid state. The [N–H···O] hydrogen bonds have the following distances and angles: [N···O] 3.10, 3.05, 3.00 Å, [H···O] 2.25, 2.39, 2.33 Å, [N–H···O] 155, 133, 131°. The [C–H···O] hydrogen bonds have the following distances and angles: [C···O] 3.24 Å, [H···O] 2.30 Å, [C–H···O] 163°.

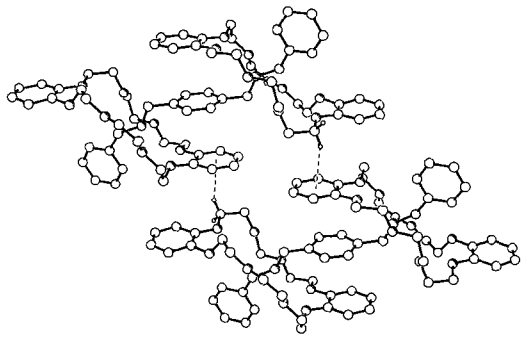

Fig. 36. The linking of 2:1 complexes, $[(\mathbf{DB24C8})_2 \cdot \mathbf{4}\text{-}H_2]^{2+}$, in the crystallographic *a* direction through [C–H···π] interactions.

8. α,α′-Bisbenzylammonium-*p*-xylene Bis(hexafluorophosphate) ($\mathbf{4}\text{-}H_2 \cdot [PF_6]_2$) and Asym-Dibenzo[24]crown-8 (asym-DB24C8): Since **DB24C8** complexes with the dication $\mathbf{4}\text{-}H_2^{2+}$ we might expect that asym-**DB24C8** should also be a suitable host for this particular guest. This is indeed the case. A ^{1}H NMR spectrum of a 2:1 mixture of asym-**DB24C8** and $\mathbf{4}\text{-}H_2 \cdot [PF_6]_2$, recorded in CD_3CN at room temperature, provides evidence for a complicated mixture of four species—free asym-**DB24C8** and free $\mathbf{4} \cdot (HPF_6)_2$, as well as 1:1 and 2:1 complexes—being formed between the host and guest. A spectrum recorded in $CD_3CN/CDCl_3$, with 10 molar equivalents of asym-**DB24C8** relative to the dication, shows predominantly two of these species (Fig. 37)—the 2:1 complex and excess of the free crown ether. By integration of the appropriate signals, the stoichiometry of the complex was confirmed to be 2:1 (host:guest). A peak in the FAB mass spectrum at *m/z* 1360 corresponding to the 2:1 complex, after loss of one of its PF_6^- counterions, was detected (Fig. 38), along with the base peak in the spectrum at *m/z* 765 for a 1:1 complex having lost its two counterions.

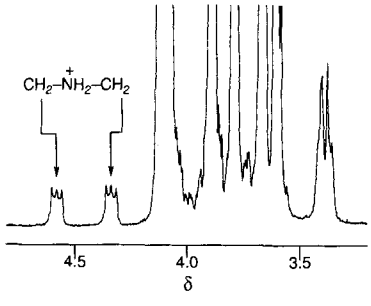

Fig. 37. The ^{1}H NMR spectrum of a 10:1 mixture of asym-**DB24C8** and $\mathbf{4}\text{-}H_2 \cdot [PF_6]_2$ in $CDCl_3/CD_3CN$ (1:1). The excess of crown ether and the nonpolar solvent results in a situation in which two major species are present—the 2:1 complex, $[(\text{asym-}\mathbf{DB24C8})_2 \cdot \mathbf{4}\text{-}H_2][PF_6]_2$, and excess of the uncomplexed asym-**DB24C8**.

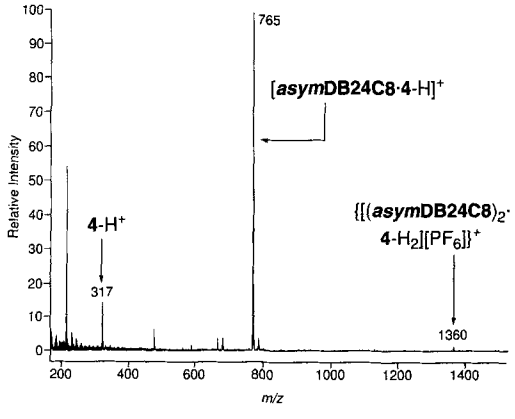

Fig. 38. The FAB mass spectrum of crystals grown of the 2:1 complex, $[(\text{asym-}\mathbf{DB24C8})_2 \cdot \mathbf{4}\text{-}H_2][PF_6]_2$.

The X-ray structural analysis confirms that both in solution and in the solid state a 2:1 complex is formed with the *N,N′*-dibenzyl-*p*-xylenediammonium dication ($\mathbf{4}\text{-}H_2^{2+}$) threaded through the centers of two asym-**DB24C8** macrocycles (Fig. 39). The dication has an *anti* geometry with the central

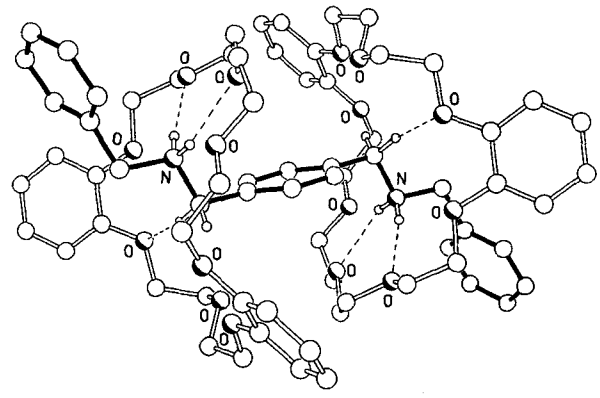

Fig. 39. Ball-and-stick representation of the 2:1 complex formed between asym-**DB24C8** and $\mathbf{4}\text{-}H_2^{2+}$ in the solid state. The [N–H···O] hydrogen bond geometries are: [N···O] 2.83, 2.91 Å; [H···O] 1.97, 2.22 Å; and [N–H···O] 160, 164°, respectively. The [C–H···O] hydrogen bond geometry is [C···O] 3.33 Å, [H···O] 2.42 Å, [C–H···O] 158°.

p-xylyl ring positioned on a crystallographic symmetry center. The geometry of each $PhCH_2NH_2^+CH_2C_6H_4$ unit is very similar to that observed for the monocation in the 1:1 complex involving [asym-**DB24C8·2**-H]$^+$. In the 2:1 complex, the two phenyl rings are approximately orthogonal (72 and 90°) to the C-CH_2-NH_2^+-CH_2-C backbone with their associated phenyl and phenylene rings folded over the longer of the two polyether linkages. It is noteworthy that, in the 2:1 complex, the conformation of the long polyether linkage reverts to a "normal" all-*gauche* geometry. The 2:1 complex is stabilized by pairs of both [N–H···O] and [C–H···O] hydrogen bonds; the former are directed toward the second and third oxygen atoms of the long polyether linkage (cf. the second and fourth oxygen atoms in the 1:1 [asym-**DB24C8·2**-H]$^+$ complex), whilst the latter occurs between one of each of the *p*-xylyl methylene CH groups of the dication and one of the catechol oxygen atoms within each asym-**DB24C8**. Noticeably, significant intercomplex [π···π] and [C–H···π] interactions are absent. There is a marginal intercomplex interaction involving the benzyl rings of the dication within one complex and one of the catechol rings of another complex. This interaction involves a minimal overlap between approximately parallel ring systems (12° interring tilt angle) with a ring centroid/ring centroid separation of 4.08 Å and a mean interplanar separation of 3.18 Å.

Conclusions and Reflections

Our tour of the secondary dialkylammonium salt complexes has come full circle (Fig. 40). We began by looking at four 1:1 complexes between monocationic salts and small crown ethers: then we extended the size of the macrocycle to accommodate two ammonium salts and formed a 1:2 complex, we added a second cationic recognition site for the macrocycle and formed a 2:2 complex, and finally we reduced the macrocycle down to its original size to form two 2:1 complexes. This conceptually simple line of investigation has produced some fascinating su-

0947-6539/96/0206-0724 $ 15.00+.25/0 Chem. Eur. J. 1996, 2, No. 6

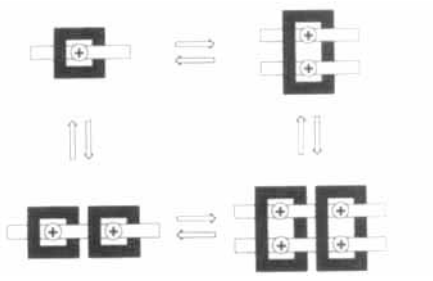

Fig. 40. Cartoon representations of the types of pseudorotaxanes described in this paper. By enlarging or reducing the size of the crown ether rings (black rings) or by adding or removing NH_2^+ centers (+) in the threadlike components (white bars) we have managed to prepare examples of all four of these supermolecules of varying stoichiometries.

perstructures, proving that crown ether chemistry, although associated very much with the beginnings of the ever-expanding science of supramolecular chemistry, is still capable of producing quite spectacular results. That something as simple as binding secondary dialkylammonium ions with the "first" macrocyclic polyethers is only now being explored after nearly thirty years of crown ether chemistry, shows that important new discoveries can still be made by looking at very simple supramolecular systems.

Experimental Procedure

Materials and Methods: **DB24C8** was purchased from Aldrich. Asym-**DB24C8** [1] and **BPP34C10** [36] were prepared according to literature procedures. Other chemicals were purchased from Aldrich and used without further purification. Solvents were either employed as purchased or dried according to procedures described in the literature. Melting points were determined on an Electrothermal 9200 apparatus and are uncorrected. ^{1}H NMR spectra were recorded on either a Bruker AC300 (300 MHz) spectrometer or a Bruker AMX400 (400 MHz) spectrometer with either the solvent as reference or TMS as the internal standard. ^{13}C NMR spectra were recorded on a Bruker AC300 (75.5 MHz) spectrometer using the JMOD pulse sequence. All chemical shifts are quoted on the δ scale. All coupling constants are expressed in Hertz (Hz). Fast atom bombardment mass spectra (FABMS) were obtained from a Kratos MS80RF mass spectrometer coupled to an off-line Sun workstation for processing raw-data experiments. The atom gun was an adapted saddle-field source (Ion Tech) operating at 7 keV with a tube current of ca. 2 mA. Krypton was used to provide a primary beam of atoms, and samples of the molecules were dissolved in a small volume (ca. 1–2 μL) of *m*-nitrobenzyl alcohol and loaded on to a stainless steel probe tip. Spectra were recorded in the positive-ion mode at a scan speed of 10 s per decade. Liquid secondary-ion mass spectra (LSIMS) were obtained from a VG Zabspec mass spectrometer using a *m*-nitrobenzyl alcohol matrix and operating in the positive-ion mode at a scan speed of 5 s per decade. Microanalyses were performed by the University of Sheffield Microanalytical Service.

General Procedure for the Synthesis of [R_2NH_2][PF_6] Salts: HCl (2 M, 250 mL) was added to R_2NH (ca. 25 mmol), and the solution stirred for 4 h. Solvent was removed under vacuum and the residue dissolved in H_2O (100 mL). Saturated aqueous NH_4PF_6 was added until no further precipitation occurred. The white solid was filtered off and dried.

Di-*n*-butylammonium Hexafluorophosphate (**1**-H·PF_6): Yield 92%; m.p. 187–188 °C; MS (CI): *m/z* 130 [$M - PF_6$]$^+$; ^{1}H NMR (300 MHz, $CDCl_3$): δ = 0.97 (t, J = 7.5 Hz, 6H; CH_3), 1.36–1.48 (m, 4H; γ-CH_2), 1.74–1.85 (m, 4H; β-CH_2), 2.96–3.05 (m, 4H; α-CH_2), 7.65 (brs, 2H; NH_2); ^{13}C NMR (75 MHz, $CDCl_3$): δ = 13.5 (CH_3), 19.9 (γ-CH_2), 27.6 (β-CH_2), 47.6 (α-CH_2); calcd for $C_8H_{20}NPF_6$: C 34.91, H 7.27, N 5.09%; found: C 35.03, H 7.39, N 5.11%.

Dibenzylammonium Hexafluorophosphate (**2**-H·PF_6): Yield 91%; m.p. 205–208 °C; MS (FAB): *m/z*: 198 [$M - PF_6$]$^+$; ^{1}H NMR (300 MHz, CD_3SOCD_3): δ = 4.20 (s, 4H; CH_2), 7.39–7.53 (m, 10H; aromatic protons), 9.19 (brs, 2H; NH_2); ^{13}C NMR (75 MHz, CD_3SOCD_3): δ = 50.3 (CH_2), 128.8 (aromatic CH), 129.1 (aromatic CH), 130.0 (aromatic CH), 131.9 (*ipso*-C); calcd for $C_{14}H_{16}NPF_6$: C 48.98, H 4.66, N 4.08%; found: C 48.72, H 4.53, N 4.28%.

Benzyl-*n*-butylammonium Hexafluorophosphate (**3**-H·PF_6): Yield 67%; m.p. 155–158 °C; MS (FAB): *m/z* 473 [2$M - PF_6$]$^+$, 164 [$M - PF_6$]$^+$; ^{1}H NMR (300 MHz, CD_3CN): δ = 0.93 (t, J = 7.5 Hz, 3H; CH_3), 1.37 (m, 2H; γ-CH_2), 1.63 (m, 2H; β-CH_2), 3.01 (m, 2H; α-CH_2), 4.15 (s, 2H; benzylic CH_2), 7.48 (s, 5H; aromatic protons); ^{13}C NMR (75 MHz, CD_3CN): δ = 13.7 (CH_3), 19.6 (γ-CH_2), 28.0 (β-CH_2), 48.5 (α-CH_2), 52.2 (benzylic CH_2), 128.9 (*ipso*-C), 130.0 (aromatic CH), 130.6 (aromatic CH), 131.0 (aromatic CH). Calcd for $C_{11}H_{18}NPF_6$: C 42.73, H 5.87, N 4.53%; found C 42.59, H 5.81, N 4.70%.

α,α′-Bisbenzylammonium-*p*-xylene Bis(hexafluorophosphate) (**4**-H_2·$[PF_6]_2$): A solution of benzylamine (5.14 g, 0.048 mmol) and terephthaldehyde (3.26 g, 0.024 mol) was heated under reflux in toluene (200 mL) with stirring in a Dean–Stark apparatus for 10 h. After the reaction mixture had been allowed to cool down to room temperature, the solvent was evaporated off under vacuum to give the 1,4-bis(benzyliminomethyl)benzene as a brown solid [^{1}H NMR ($CDCl_3$, 300 MHz): δ = 4.84 (s, 4H; NCH_2), 7.18–7.47 (m, 10H; C_6H_5), 7.82 (s, 4H; C_6H_4), 8.41 (s, 2H; N=CH)], which was dissolved in MeOH (50 mL). $NaBH_4$ (3.80 g, 0.10 mol) was added in small portions to the reaction mixture, which was heated under reflux with stirring for 8 h. It was then allowed to cool down to room temperature and concentrated HCl was added (pH < 2). After evaporation of the solvent, the residue was suspended in H_2O (30 mL) and extracted with CH_2Cl_2 (4 × 30 mL). The combined extracts were washed with 5% aqueous $NaHCO_3$ (2 × 60 mL) and H_2O (50 mL), and the dried ($MgSO_4$). Removal of the solvent under vacuum afforded 1,4-bis(benzyaminomethyl)benzene (4.00 g) as a colorless solid [^{1}H NMR (300 MHz, $CDCl_3$): δ = 3.80 (s, 4H; NCH_2), 3.81 (s, 4H; NCH_2), 7.15–7.45 (m, 14H; aromatic protons)] of which 2.00 g (0.006 mol) was dissolved in MeOH (30 mL). Concentrated HCl was added (pH < 2), and the reaction mixture was stirred for a further hour. Evaporation of the solvent afforded a colorless solid, which was suspended in Me_2CO (30 mL). An aqueous solution of NH_4PF_6 was added until dissolution occurred. Evaporation of Me_2CO afforded colorless crystals of **4**-H_2·$[PF_6]_2$, which were isolated, washed with H_2O, and air-dried (3.50 g, 90%, m.p. 238 °C with decomp.). MS (FAB): *m/z* 463 [$M - PF_6$]$^+$; ^{1}H NMR (300 MHz, CD_3CN): δ = 4.24 (s, 4H; N^+CH_2), 4.25 (s, 4H; N^+CH_2), 7.45–7.51 (m, 10H; C_6H_5), 7.52 (s, 4H; C_6H_4); ^{13}C NMR (CD_3CN): δ = 51.6 (N^+CH_2), 52.4 (N^+CH_2), 129.9, 130.6, 131.0, 131.2, 131.6, 132.9. An analytical sample was obtained of the dihydrochloride salt **4**-H_2·2Cl: calcd for $C_{22}H_{26}N_2Cl_2$: C 67.88, H 6.68, N 7.19%; found C 67.74, H 6.57, N 7.13%.

[**DB24C8**·**1**-H][PF_6]: Single crystals suitable for X-ray crystallography were grown by liquid diffusion of *n*-hexane into an equimolar solution of **DB24C8** and **1**-H·PF_6 in $CHCl_3$.

[**DB24C8**·**2**-H][PF_6]: Single crystals suitable for X-ray crystallography were grown by liquid diffusion of *n*-hexane into an equimolar solution of **DB24C8** and **2**-H·PF_6 in $CHCl_3$.

[Asym-**DB24C8**·**2**-H][PF_6]: Single crystals suitable for X-ray crystallography were grown by liquid diffusion of *n*-hexane into an equimolar solution of asym-**DB24C8** and **2**-H·PF_6 in $CHCl_3$.

[**DB24C8**·**3**-H][PF_6]: Single crystals suitable for X-ray crystallography were grown by liquid diffusion of *n*-hexane into an equimolar solution of **DB24C8** and **3**-H·PF_6 in $CHCl_3$.

[**BPP34C10**·(**2**-H)$_2$][$PF_6]_2$: Single crystals suitable for X-ray crystallography were grown by liquid diffusion of *n*-pentane into an equimolar solution of **BPP34C10** and **2**-H·PF_6 in Me_2CO. Needles of **BPP34C10** were also formed initially from this mixture, hinting that the complex would have more than one equivalent of **2**-HPF_6 in the crystal.

[(**BPP34C10**)$_2$·(**4**-H_2)$_2$][$PF_6]_4$: Single crystals suitable for X-ray crystallography were grown by liquid diffusion of *n*-pentane into an equimolar solution of **BPP34C10** and **4**-H_2·2PF_6 in Me_2CO.

[(**DB24C8**)$_2$·**4**-H_2][$PF_6]_2$: Single crystals suitable for X-ray crystallography were grown by vapor diffusion of diisopropyl ether into a 2:1 molar ratio solution of **DB24C8** and **4**-H_2·2PF_6 in MeCN.

[(Asym-**DB24C8**)$_2$·**4**-H_2][$PF_6]_2$: Single crystals suitable for X-ray crystallography were grown by vapor diffusion of diisopropyl ether into a 2:1 molar ratio solution of asym-**DB24C8** and **4**-H_2·2PF_6 in MeCN.

X-Ray Crystallography: Further details of the crystal structure investigations for complexes [**DB24C8**·**1**-H][PF_6] and [**DB24C8**·**2**-H][PF_6], and for complexes [**BPP34C10**·(**2**-H)$_2$][$PF_6]_2$, [(**BPP34C10**)$_2$·(**4**-H_2)$_2$][$PF_6]_4$, and [(**DB24C8**)$_2$·**4**-H_2][$PF_6]_2$ may be obtained from the Cambridge Crystallographic Data Centre at the address given below, on quoting references [24] and [25], respectively.
The crystallographic data (excluding structure factors) for the structures reported in Table 5 have been deposited with the Cambridge Crystallographic Data Centre as supplementary publication no. CCDC-1220-7. Copies of the data can be obtained free of charge on application to The Director, CCDC, 12 Union Road, Cambridge CB21EZ, UK (Fax: Int. code +(1223)336-033; e-mail: teched@chemcrys.cam.ac.uk).

Table 5. Crystallographic data [a].

	[asym-**DB24C8**·**2**-H][PF_6]	[**DB24C8**·**3**-H][PF_6]	[(asym-**DB24C8**)$_2$·**4**-H_2][PF_6]$_2$
empirical formula [b]	$C_{38}H_{48}NO_8 \cdot PF_6$	$C_{35}H_{50}NO_8 \cdot PF_6$	$C_{70}H_{90}N_2O_{16} \cdot 2PF_6$
solvent	N/A	N/A	2MeCN
M_r	791.7	757.7	1587.5
color, habit	clear blocks	clear blocks	clear rhombi
crystal size/mm	$0.50 \times 0.37 \times 0.33$	$0.67 \times 0.57 \times 0.50$	$0.20 \times 0.20 \times 0.20$
T/K	293	293	223
crystal system	triclinic	orthorhombic	triclinic
space group	$P\bar{1}$	*Pbca*	$P\bar{1}$
a/Å	11.286(3)	15.860(6)	12.408(3)
b/Å	13.611(2)	30.548(10)	12.517(3)
c/Å	14.056(3)	32.344(16)	13.467(5)
α/°	106.47(2)	90	75.17(2)
β/°	99.36(2)	90	79.37(2)
γ/°	91.02(2)	90	76.56(2)
V/Å^3	2038.4(7)	15670(11)	1949.0(9)
Z	2	16 [c]	1 [d]
D_c/g cm^{-3}	1.290	1.285	1.353
radiation	$Cu_{K\alpha}$ [e]	$Cu_{K\alpha}$	$Cu_{K\alpha}$ [e]
μ/mm^{-1}	1.268	1.292	1.334
$F(000)$	832	6400	834
2θ range/°	3–120	3–116	7–122
independent reflections	6039	10913	5960
observed reflections [$F_o > 4\sigma(\|F_o\|)$]	4357	4103	5225
no. of parameters	524	551	492
g in weighting scheme [f]	0.0005	0.0005	0.0704, 1.5988 [g]
extinction, χ	0.0074	N/A	0.0030
final R (R_w)	0.095 (0.103)	0.141 (0.143)	0.052 (0.138) [h]
Largest and mean Δ/σ	0.557, 0.037	0.332, 0.008	0.166, 0.007
data/parameter ratio	8.31	7.45	10.62
largest difference peak, hole/e Å^{-3}	0.31, −0.33	0.67, −0.49	0.49, −0.58

[a] Details in common: graphite monochromated $Cu_{K\alpha}$ radiation, ω scans, Siemens P4/PC diffractometer, refinement based on F. [b] Excluding solvent. [c] There are two crystallographically independent molecules in the asymmetric unit. [d] The molecule has crystallographic C_i symmetry. [e] Siemens P4/RA diffractometer. [f] $w^{-1} = \sigma^2(F) + gF^2$. [g] Refinement based on F^2; the values given are a and b in $w^{-1} = \sigma^2(F_o^2) + (aP)^2 + bP$. [h] The value in parentheses is for $wR_2 = \sqrt{\{\sum[w(F_o^2 - F_c^2)^2]/\sum[w(F_o^2)^2]\}}$.

Table 5 provides a summary of the crystal data, data collection, and refinement parameters for complexes [**DB24C8**·**3**-H][PF_6], [asym-**DB24C8**·**2**-H][PF_6], and [(asym-**DB24C8**)$_2$·**4**-H_2][PF_6]$_2$. In [asym-**DB24C8**·**2**-H][PF_6] there is 50:50 disorder in the PF_6^- anion. All non-hydrogen atoms in this structure were refined anisotropically. The positions of the hydrogen atoms were determined from ΔF maps and subsequently idealized and refined isotropically (riding model). [**DB24C8**·**3**-H][PF_6] contains two crystallographically independent 1:1 complexes. In one complex, there is 75:25 disorder in the position of the terminal methyl group of the benzyl-*n*-butylammonium cation **3**$^+$. One of the PF_6^- anions is also disordered, 70:30. Hydrogen atoms were handled as in [asym-**DB24C8**·**2**-H][PF_6]. Because of the limited number of observed data, only the major occupancy P and F atoms, and the heteroatoms of the 1:1 complexes, were refined anisotropically; the remaining non-hydrogen atoms and minor occupancy F atoms were refined isotropically. In the 2:1 complex [(asym-**DB24C8**)$_2$·**4**-H_2][PF_6]$_2$, which was determined at low temperature (−50 °C), the PF_6^- anion exhibits 60:40 disorder. All major occupancy non-hydrogen atoms were refined anisotropically. Hydrogen atoms were handled as for the 1:1 complexes [asym-**DB24C8**·**2**-H][PF_6] and [**DB24C8**·**3**-H][PF_6]. Computations were carried out using the SHELXTL program system [61].

Acknowledgements: This research, which was sponsored in the UK by the ZENECA Strategic Research Fund, was supported additionally by the Biotechnology and Biological Sciences Research Council and Engineering and Physical Sciences Research Council. We thank Dr Andrew Collins of ZENECA Specialties (Blackley) for helpful discussions.

Received: December 13, 1995 [F260]

[1] C. J. Pedersen, *J. Am. Chem. Soc.* **1967**, *89*, 7017–7036.

[2] a) I. Goldberg in *Inclusion Compounds, Vol. 2* (Eds.: J. L. Atwood, J. E. D. Davies, D. D. MacNicol), Academic Press, London, **1984**, 261–335; b) G. W. Gokel, *Crown Ethers and Cryptands*, The Royal Society of Chemistry, Cambridge, **1991**; c) D. J. Cram, K. N. Trueblood, *Top. Curr. Chem.* **1981**, *98*, 43–106; d) D. J. Cram, *Angew. Chem. Int. Ed. Engl.* **1988**, *27*, 1009–1020; e) D. J. Cram, J. M. Cram, *Container Molecules and their Guests*, The Royal Society of Chemistry, Cambridge, **1994**; f) I. O. Sutherland, *Chem. Soc. Rev.* **1986**, *15*, 63–91; g) I. O. Sutherland, *J. Chem. Soc. Faraday Trans. 1* **1986**, *82*, 1145–1159; h) I. O. Sutherland, *J. Inclusion Phenom.* **1989**, *7*, 213–226; i) I. O. Sutherland, *Pure Appl. Chem.* **1989**, *61*, 1547–1554; j) *ibid.* **1990**, *62*, 499–504; k) C. J. Pedersen, *Angew. Chem. Int. Ed. Engl.* **1988**, *27*, 1021–1027; l) J. F. Stoddart, *Chem. Soc. Rev.* **1979**, *8*, 85–142; m) J. F. Stoddart, *Top. Stereochem.* **1988**, *17*, 205–288.

[3] a) J.-M. Lehn, *Angew. Chem. Int. Ed. Engl.* **1990**, *29*, 1304–1319; b) J.-M. Lehn, *Science* **1993**, *260*, 1762–1763; c) J.-M. Lehn, *Pure Appl. Chem.* **1994**, *66*, 1961–1966; d) J.-M. Lehn, *Supramolecular Chemistry: Concepts and Perspectives*, VCH, Weinheim, **1995**.

[4] a) R. M. Izatt, B. L. Nielsen, J. J. Christensen, J. D. Lamb, *J. Membrane Sci.* **1981**, *9*, 263–271; b) R. L. Bruening, R. M. Izatt, J. S. Bradshaw, in *Cation Binding by Macrocycles* (Eds.: Y. Inoue, G. W. Gokel), Marcel Dekker, New York, **1990**, 111–132; c) M. T. Reetz, J. Huff, J. Rudolf, K. Töllner, A. Deege, R. Goddard, *J. Am. Chem. Soc.* **1994**, *116*, 11588–11589.

[5] R. M. Izatt, T. Wang, J. K. Hathaway, X. X. Zhang, J. C. Curtis, J. S. Bradshaw, C. Y. Zhu, P. Huszthy, *J. Inclusion Phenom.* **1994**, *17*, 157–175 and references therein.

[6] a) O. Nagano, A. Kobayashi, Y. Sasaki, *Bull. Chem. Soc. Jpn.* **1978**, *51*, 790–793; b) D. A. Pears, J. F. Stoddart, M. E. Fakley, B. L. Allwood, D. J. Williams, *Acta. Crystallogr.* **1988**, *C44*, 1426–1430.

[7] a) M. J. Bovill, D. J. Chadwick, I. O. Sutherland, D. Watkin, *J. Chem. Soc. Perkin Trans. 2* **1980**, 1529–1543; b) J. M. Maud, J. F. Stoddart, D. J. Williams, *Acta Crystallogr.* **1985**, *C41*, 137–140; c) K. N. Trueblood, C. B. Knobler, D. S. Lawrence, R. V. Stevens, *J. Am. Chem. Soc.* **1982**, *104*, 1355–1362.

[8] Y. L. Ha, A. K. Chakraborty, *J. Phys. Chem.* **1992**, *96*, 6410–6417.

[9] M. Newcomb, S. S. Moore, D. J. Cram, *J. Am. Chem. Soc.* **1977**, *99*, 6405–6410.

[10] a) R. M. Izatt, K. Pawlak, J. S. Bradshaw, R. L. Bruening, *Chem. Rev.* **1991**, *91*, 1721–2085; b) *ibid.* **1995**, *95*, 2529–2586.

[11] S. Ganguly, H. W. Gibson, *Macromolecules* **1993**, *26*, 2408–2412.

[12] a) J. S. Bradshaw, S. L. Baxter, J. D. Lamb, R. M. Izatt, J. J. Christensen, *J. Am. Chem. Soc.* **1981**, *103*, 1821-1827; b) M. Newcomb, J. M. Timko, D. M. Walba, D. J. Cram, *ibid.* **1977**, *99*, 6392–6398; c) R. C. Hegelson, T. L. Tarnowski, J. M. Timko, D. J. Cram, *ibid.* **1977**, *99*, 6411–6418; d) J. M. Timko, S. S. Moore, D. M. Walba, P. C. Hiberty, D. J. Cram, *ibid.* **1977**, *99*, 4207–4219; e) J.-M. Lehn, P. Vierling, R. C. Hayward, *J. Chem. Soc. Chem. Commun.* **1979**, 296–298; f) R. Aldag, G. Schröder, *Liebigs Ann. Chem.* **1984**, 1036–1045; g) R. Ellinghaus, G. Schröder, *ibid.* **1985**, 418–420.

[13] a) J. C. Metcalfe, J. F. Stoddart, G. Jones, T. Crawshaw, E. Gavuzzo, D. J. Williams, *J. Chem. Soc. Chem. Commun.* **1981**, 432–434; b) M. J. Bovill, D. J. Chadwick, M. R. Johnson, N. F. Jones, I. O. Sutherland, R. F. Newton, *ibid.* **1979**, 1065–1066; c) N. K. Dalley, J. S. Bradshaw, S. B. Larson, S. H. Simonsen, *Acta Crystallogr.* **1982**, *B38*, 1859–1862.

[14] S. Misumi, *Top. Curr. Chem.* **1993**, *165*, 163–192 and references therein.

[15] T. Kaneda, S. Umeda, Y. Ishizaki, H.-S. Kuo, S. Misumi, Y. Kai, N. Kanehisa, N. Kasai, *J. Am. Chem. Soc.* **1989**, *111*, 1881–1883.

[16] T. Kaneda, Y. Ishizaki, S. Misumi, Y. Kai, G. Hirao, N. Kasai, *J. Am. Chem. Soc.* **1988**, *110*, 2970–2972.

[17] S. Misumi, *Pure Appl. Chem.* **1990**, *62*, 493–498.

[18] F. Vögtle, R. Hoss, *J. Chem. Soc. Chem. Commun.* **1992**, 1584–1585.

[19] R. M. Izatt, J. D. Lamb, N. E. Izatt, B. E. Rossiter, Jr., J. J. Christensen, B. L. Haymore, *J. Am. Chem. Soc.* **1979**, *101*, 6273–6276.

[20] J. C. Metcalfe, J. F. Stoddart, G. Jones, *J. Am. Chem. Soc.* **1977**, *99*, 8317–8319.

[21] J. Krane, O. Aune, *Acta Chem. Scand.* **1980**, *B34*, 397–401.

[22] H. Tsukube, *Bull. Chem. Soc. Jpn.* **1984**, *57*, 2685–2686.

[23] S. S. Abed-Ali, B. J. Brisdon, R. England, *J. Chem. Soc. Chem. Commun.* **1987**, 1565–1566.

[24] P. R. Ashton, P. J. Campbell, E. J. T. Chrystal, P. T. Glink, S. Menzer, D. Philp, N. Spencer, J. F. Stoddart, P. A. Tasker, D. J. Williams, *Angew. Chem.* **1995**, *107*, 1997–2001; *Angew. Chem. Int. Ed. Engl.* **1995**, *34*, 1865–1869.

[25] P. R. Ashton, E. J. T. Chrystal, P. T. Glink, S. Menzer, C. Schiavo, J. F. Stoddart, P. A. Tasker, D. J. Williams, *Angew. Chem.* **1995**, *107*, 2001–2004; *Angew. Chem. Int. Ed. Engl.* **1995**, *34*, 1869–1871.

[26] C. B. Aakeröy, K. R. Seddon, *Chem. Soc. Rev.* **1993**, *22*, 397–407.

[27] Pseudorotaxanes have been defined as inclusion complexes in which a threadlike molecule is encircled by one or more ringlike molecules in such a way that the two ends of the thread are projected away from the center of the ring. In a rotaxane (Latin *rota*, wheel; *axis*, axle), the two ends of the thread are terminated by bulky groups which do not allow the passage of the ring—thus, the two (or more) components are mutually interlocked. The prefix pseudo denotes that in a pseudorotaxane the two components are not interlocked, but instead are free to dissociate because the end groups are small enough to allow passage of the ring. See, for example, ref. [28].

[28] a) P. L. Anelli, P. R. Ashton, A. M. Z. Slawin, N. Spencer, J. F. Stoddart, D. J. Williams, *Angew. Chem. Int. Ed. Engl.* **1991**, *30*, 1036–1039; b) P. R. Ashton, D. Philp, N. Spencer, J. F. Stoddart, *J. Chem. Soc. Chem. Commun.* **1991**, 1677–1679; c) P. R. Ashton, D. Philp, M. V. Reddington, A. M. Z. Slawin, N. Spencer, J. F. Stoddart, D. J. Williams, *ibid.* **1991**, 1680–1683; d) P. R. Ashton, D. Philp, N. Spencer, J. F. Stoddart, D. J. Williams, *J. Chem. Soc. Chem. Commun.* **1994**, 181–184.

[29] a) H. Sleiman, P. Baxter, J.-M. Lehn, *J. Chem. Soc. Chem. Commun.* **1995**, 715–716; b) J. C. Chambron, C. Dietrich-Buchecker, J. J. Nierengarten, J.-P. Sauvage, N. Solladie, A. M. Albrecht-Gary, M. Meyer, *New J. Chem.* **1995**, *19*, 409–426.

[30] Reviews: a) G. Schill, *Catenanes, Rotaxanes and Knots*, Academic Press, New York, **1971**; b) C. O. Dietrich-Buchecker, J.-P. Sauvage, *Bioorganic Chemistry Frontiers* **1991**; *2*, 195–248; c) H. W. Gibson, M. C. Bheda, P. T. Engen, *Prog. Polym. Sci.* **1994**, *19*, 843–945; d) D. B. Amabilino, J. F. Stoddart, *Chem. Rev.* **1995**, *95*, 2725–2828. For three recent representative examples, see: e) E. Córdova, R. Bissell, A. E. Kaifer, *J. Org. Chem.* **1995**, *60*, 1033–1038; f) F. Diederich, C. Dietrich-Buchecker, J.-F. Nierengarten, J.-P. Sauvage, *J. Chem. Soc. Chem. Commun.* **1995**, 781–782; g) F. Vögtle, M. Händel, S. Meier, S. Ottens-Hildebrandt, F. Ott, T. Schmidt, *Liebigs Ann.* **1995**, 739–743.

[31] A. P. de Silva, C. P. McCoy, *Chem. Ind.* **1994**, 992–996.

[32] R. A. Bissell, E. Córdova, A. E. Kaifer, J. F. Stoddart, *Nature (London)* **1994**, *369*, 133–137.

[33] a) P. L. Anelli, N. Spencer, J. F. Stoddart, *J. Am. Chem. Soc.* **1991**, *113*, 5131–5133; b) P. R. Ashton, D. Philp, N. Spencer, J. F. Stoddart, *J. Chem. Soc. Chem. Commun.* **1992**, 1124–1128; c) P. R. Ashton, R. A. Bissell, N. Spencer, J. F. Stoddart, M. S. Tolley, *Synlett* **1992**, 914–918; d) P. R. Ashton, R. A. Bissell, R. Górski, D. Philp, N. Spencer, J. F. Stoddart, M. S. Tolley, *ibid.* **1992**, 919–922; e) P. R. Ashton, R. A. Bissell, N. Spencer, J. F. Stoddart, M. S. Tolley, *ibid.* **1992**, 923–926; f) A. C. Benniston, A. Harriman, V. M. Lynch, *J. Am. Chem. Soc.* **1995**, *117*, 5275–5291.

[34] A. G. Kolchinski, D. H. Busch, N. W. Alcock, *J. Chem. Soc. Chem. Commun.* **1995**, 1289–1291.

[35] P. R. Ashton, P. T. Glink, J. F. Stoddart, P. A. Tasker, A. J. P. White, D. J. Williams, *Chem. Eur. J.* **1996**, *2*, 729–736.

[36] a) P. L. Anelli, P. R. Ashton, R. Ballardini, V. Balzani, M. Delgado, M. T. Gandolfi, T. T. Goodnow, A. E. Kaifer, D. Philp, M. Pietraszkiewicz, L. Prodi, M. V. Reddington, A. M. Z. Slawin, N. Spencer, J. F. Stoddart, C. Vicent, D. J. Williams, *J. Am. Chem. Soc.* **1992**, *114*, 193–218; b) D. B. Amabilino, P. R. Ashton, C. L. Brown, E. Córdova, L. A. Godínez, T. T. Goodnow, A. E. Kaifer, S. P. Newton, M. Pietraszkiewicz, D. Philp, F. M. Raymo, A. S. Reder, M. T. Rutland, A. M. Z. Slawin, N. Spencer, J. F. Stoddart, D. J. Williams, *ibid.* **1995**, *117*, 1271–1293; c) D. B. Amabilino, P. L. Anelli, P. R. Ashton, G. R. Brown, E. Córdova, L. A. Godinez, W. Hayes, A. E. Kaifer, D. Philp, A. M. Z. Slawin, N. Spencer, J. F. Stoddart, M. S. Tolley, D. J. Williams, *ibid.* **1995**, *117*, 11142–11170; d) P. R. Ashton, R. Ballardini, V. Balzani, A. Credi, M. T. Gandolfi, S. Menzer, L. Pérez-García, L. Prodi, J. F. Stoddart, M. Venturi, A. J. P. White, D. J. Williams, *ibid.* **1995**, *117*, 11171–11197.

[37] This situation may not be too surprising since the dialkylammonium ions are charged and need not be protonated by the matrix upon fast atom bombardment. Thus, peaks corresponding to the dialkylammonium ions and their (stronger) complexes may be expected to be more intense than those for protonated, but uncomplexed, crown ethers.

[38] O. Kennard, *Supramol. Chem.* **1993**, *1*, 277–295.

[39] CPK space-filling molecular models indicate that an alkyl group would have relatively little difficulty in threading through this macrocycle, and so we would probably expect fast exchange to occur in solution between complexed and uncomplexed species at room temperature on the ^{1}H NMR timescale at 400 MHz.

[40] The $\Delta\delta$ values for the α-CH_2, β-CH_2, γ-CH_2 and Me protons from the ^{1}H NMR spectra recorded on **1**·H·PF_6 and [**DB24C8**·**1**-H]·[PF_6] at 300 MHz in $CDCl_3$ are +0.19, −0.30, −0.25, and −0.23 ppm, respectively.

[41] a) Z. D. Hill, P. MacCarthy, *J. Chem. Educ.* **1986**, *63*, 162–167; b) K. A. Connors, *Binding Constants*, Wiley-Interscience, New York, **1987**; c) C. S. Wilcox in *Frontiers in Supramolecular Organic Chemistry and Photochemistry*, (Eds.: H.-J. Schneider, H. Dürr), VCH, Weinheim, **1991**, 123–143; d) T. Wang, J. S. Bradshaw, R. M. Izatt, *J. Heterocycl. Chem.* **1994**, *31*, 1097–1114.

[42] The Eyring equation was employed to obtain $\Delta G_c^{\ddagger}$ values at the coalescence temperature T_c, where the rate constant can be calculated (I. O. Sutherland, *Ann. Rep. NMR Spectrosc.* **1971**, *4*, 71–235) from the approximate expression, $k_c = (\pi\Delta\nu)/(2^{1/2})$, where k_c is the first-order rate constant at T_c and $\Delta\nu$ is the limiting chemical shift difference (in Hz) between the coalescing signals in the absence of exchange.

[43] The signal for the resonance of the benzylic methylene protons appears as a second-order multiplet as a result of coupling to the NH_2^+ protons associated with the dialkylammonium ion center in the complex. This coupling was confirmed by a D_2O exchange experiment, which resulted in exchange of the NH_2^+ protons and a consequent collapse of the multiplet for benzylic methylene protons into a broad singlet. Presumably, this coupling results from the "freezing out" of the exchange of the NH_2^+ protons—with H_2O present in the solvent—once the dialkylammonium ion center is encircled by the crown ether.

[44] a) C. A. Hunter, J. K. M. Sanders, *J. Am. Chem. Soc.* **1990**, *112*, 5525–5534; b) C. A. Hunter, *Chem. Soc. Rev.* **1994**, *23*, 101–109.

[45] a) D. B. Amabilino, I. W. Parsons, J. F Stoddart, *Trends. Polym. Sci.* **1994**, *2*, 146–152; b) X. Sun, D. B. Amabilino, P. R. Ashton, I. W. Parsons, J. F. Stoddart, M. S. Tolley, *Macromol. Symp.* **1994**, *77*, 191–207; c) P. R. Ashton, J. A. Preece, J. F. Stoddart, M. S. Tolley, *Synlett* **1994**, 789–792; d) J. A. Preece, J. F. Stoddart, *Macromol. Symp.* **1995**, *98*, 527–540; e) P. R. Ashton, J. Huff, S. Menzer, I. W. Parsons, J. A. Preece, J. F. Stoddart, M. S. Tolley, A. J. P. White, D. J. Williams, *Chem. Eur. J.* **1996**, *2*, 31–44; f) H. W. Gibson, H. Marand, *Adv. Mater.* **1993**, *5*, 11–21; g) H. W. Gibson, S. Liu, P. Lecavalier, C. Wu, Y. X. Shen, *J. Am. Chem. Soc.* **1995**, *117*, 852–874.

[46] Polyamine/polyammonium polymers are known: a) T. Perner, R. C. Schultz, *Br. Polym. J.* **1987**, *19*, 181–188; b) G. Wenz, B. Keller, *Angew. Chem. Int. Ed. Engl.* **1992**, *31*, 197–199.

[47] A single-point K_a determination of a different kind has been reported by J. C. Adrian, Jr., C. S. Wilcox, *J. Am. Chem. Soc.* **1991**, *113*, 678–680.

[48] The Gutmann donor number provides a semiquantitative measurement of the ability of a solvent to donate its electrons in a noncovalent bond: a) V. Gutmann, E. Wychera, *Inorg. Nucl. Chem. Lett.* **1966**, *2*, 257–260; b) C. Reichardt, *Solvents and Solvent Effects in Organic Chemistry*, Second Edition, VCH, Weinheim, **1988**.

[49] M. J. Blandamer, J. Burgess, R. E. Robertson, J. M. W. Scott, *Chem. Rev.* **1982**, *82*, 259–286.

[50] Heat capacity is, by definition, the variation of ΔH° with temperature, i.e., $\Delta C_p^\circ = (\partial\Delta H^\circ/\partial T)_p$.

[51] a) D. A. Stauffer, R. E. Barrans, Jr., D. A. Dougherty, *J. Org. Chem.* **1990**, *55*, 2762–2767; b) B. W. Gung, M. A. Wolf, D. A. Mareska, C. A. Brockway, *ibid.* **1994**, *59*, 4895–4898; c) G. Weber, *J. Phys. Chem.* **1995**, *99*, 1052–1059; d) H. Naghibi, A. Tamura, J. M. Sturtevant, *Proc. Natl. Acad. Sci. USA* **1995**, *92*, 5597–5599.

[52] It seems that from the recent number of publications dealing with significant heat capacity effects in host–guest chemistry, chemists should include this effect routinely in thermodynamic studies on such systems. When one is aware of the effect a nonnegligible heat capacity can have on a van't Hoff plot (i.e., curvature), one can see this effect in the literature for a number of plots—although the data points appear to be aligned along a curve, a straight line of best fit is used with a reasonably accurate "*R*" value. See, for example,: a) K. Araki, K. Inada, H. Otsuka, S. Shinkai, *Tetrahedron* **1993**, *49*, 9465–9478; b) K. I. Goldberg, J. Y. Yan, E. M. Breitung, *J. Am. Chem. Soc.* **1995**, *117*, 6889–6896; c) J. T. Davis, S. Tirumala, J. R. Jenssen, E. Radler, D. Fabris, *J. Org. Chem.* **1995**, *60*, 4167–4176.

[53] a) J. N. Wingfield, *Inorg. Chem. Acta* **1980**, *45*, L157–L159; b) J. D. Owen, *Acta Crystallogr.* **1983**, *C39*, 861–863.

[54] This feature is reminiscent of that observed in the structure of the 1:1 complex between **DB24C8** and the $[Pt(bipy)(NH_3)_2]^{2+}$ dication in the solid state. See

H. M. Colquhoun, S. M. Doughty, J. M. Maud, J. F. Stoddart, D. J. Williams, J. B. Wolstenholme, *Isr. J. Chem.* **1985**, *25*, 15–26.

[55] The signal that corresponds to a particular *O*-methylene proton on the face of the crown ether was determined from an NOE study in which the resonances of the aromatic and methylene protons associated with the benzyl group were irradiated and found to have a greater effect on one of the two resonances for the constitutionally heterotopic *O*-methylene protons. In this manner, the signals of the OCH_aH_b groups were identified. On the same face as the benzyl group, we have: α-OCH_a, $\delta = 4.17$; β-OCH_a, $\delta = 3.85$; γ-OCH_a, $\delta = 3.05$. On the face from which the butyl group protrudes: α-OCH_b, $\delta = 4.30$; β-OCH_b, $\delta = 3.75$; γ-OCH_b, $\delta = 3.45$.

[56] a) P. R. Ashton, M. Bělohradský, D. Philp, J. F. Stoddart, *J. Chem. Soc. Chem. Commun.* **1993**, 1269–1274; b) P. R. Ashton, M. Bělohradský, D. Philp, N. Spencer, J. F. Stoddart, *ibid.* **1993**, 1274–1277; c) D. B. Amabilino, P. R. Ashton, M. Bělohradský, F. M. Raymo, J. F. Stoddart, *ibid.* **1995**, 747–750; d) D. B. Amabilino, P. R. Ashton, M. Bělohradský, F. M. Raymo, J. F. Stoddart, *ibid.* **1995**, 751–753.

[57] The $\Delta\delta$ values (with reference to the uncomplexed crown ether) for the C_6H_4, α-OCH_2, β-OCH_2, γ-OCH_2, and δ-OCH_2 protons in **BPP34C10** deduced from the ^{1}H NMR spectrum of [**BPP34C10**·(**2**-H)$_2$][PF_6]$_2$ recorded in CD_2Cl_2 are +0.18, −0.03, −0.12, −0.31, and −0.43 ppm, respectively.

[58] a) W. L. Jorgensen, D. L. Severance, *J. Am. Chem. Soc.* **1990**, *112*, 4768–4774; b) M. Nishio, M. Hirota, *Tetrahedron* **1989**, *45*, 7201–7245; c) M. Nishio, Y. Umezawa, M. Hirota, Y. Takeuchi, *ibid.* **1995**, *51*, 8665–8701.

[59] a) A. Harada, J. Li, M. Kamachi, *Nature (London)* **1994**, *370*, 126–128; b) G. Li, L. B. McGown, *Science* **1994**, *264*, 249–251.

[60] For an equimolar mixture of **BPP34C10** and **4**-H_2·2PF_6 in CD_2Cl_2/CD_3CN (3:1 v/v), $\Delta\delta$ values (with reference to the free salt) of −0.34 and −0.11 ppm, respectively, are observed in the ^{1}H NMR spectrum for the aromatic phenylene and the benzylic methylene protons associated with the bridging *para*-xylyl group in the [**4**-H_2]$^{2+}$ dication.

[61] G. M. Sheldrick, SHELXTL Versions 4.02 (1990) and 5.03 (1994), Siemens Analytical X-Ray Instruments, Madison, WI.

0947-6539/96/0206-0728 $ 15.00+.25/0